Journal of Archaeological Method and Theory
https://doi.org/10.1007/s10816-022-09598-y

A PCA-AHC Approach to Provenance Studies of Non-Ferrous Metals with Combined Pb Isotope and Chemistry Data

Céline Tomczyk[1] · **Grzegorz Żabiński**[2]

Accepted: 6 December 2022

Abstract

This paper discusses the applicability of the Principal Component Analysis-Agglomerative Hierarchical Clustering (PCA-AHC) approach to provenance studies of non-ferrous metals using combined Pb isotope and chemistry data. Pb isotopic ratios were converted to the natural abundance of individual isotopes and then to weight units. Next, all relevant variables (Pb isotopes and trace elements) were processed with PCA and AHC to examine the relationships between observations. The method is first verified on three literature-based case studies (1, 2, and 3). It is argued that, as is the case in archaeological iron provenance studies, the PCA-AHC method is also viable for non-ferrous metals. This method can greatly facilitate research, compared to conventional biplots with ratios of Pb isotopes and trace elements. Additionally, PCA-AHC can become part of the initial deposit selection process, and it can help clarify less obvious classification cases. The main problem with a practical application of this approach is insufficient deposit datasets with complete Pb isotopic and chemistry data. In such cases, it is possible to use the PCA-AHC method separately on Pb isotopic and chemistry data and then to compare and contrast results. Alternatively, the proposed approach can be used solely with Pb isotopic data. This application is shown in two additional case studies (4 and 5), which demonstrate the method's application for tracing artefacts to their parent ores using datasets with a few thousand observations.

Keywords Non-ferrous metal provenance studies · Pb isotopes · Trace elements · Multivariate statistics · PCA-AHC

✉ Grzegorz Żabiński
g.zabinski@gmail.com

Céline Tomczyk
celine.tomczyk@gmail.com

[1] Département d'Histoire de l'art et d'archéologie, Université Paris 1 Panthéon-Sorbonne, Paris, France

[2] Institute of History, Jan Długosz University in Częstochowa, Częstochowa, Poland

Published online: 14 January 2023

Introduction—Principles and Limitations of Provenance Tracing Using Lead Isotopes and/or Geochemistry

The aim of this paper is to propose an improvement in methods that have been applied so far in provenance studies of archaeological non-ferrous metals. Similar to recent developments in iron provenance research where multivariate methods have been used to process chemistry data, we discuss a multivariate approach where Pb isotopic and chemistry data are either used separately or all variables are combined into a single dataset. This is because the isotopic compositions of different ore bodies frequently overlap, and for this reason, a combination of Pb isotopic and chemistry data often produces a better distinction between ore deposits (Pernicka, 2014: 250; Baron *et al.,* 2014: 669–670; Pernicka *et al.,* 2016b: 67; Radivojević *et al.,* 2019: 139). Therefore, we chose to combine these two types of analysis in a single statistical treatment. To verify the proposed approach, we conducted three case studies using well-known literature data to compare our results with those offered in relevant studies using the traditional biplot method. Case Studies 4 and 5 examine the method's performance when applied to large datasets of more than 4500 and 2000 deposit observations respectively.

Principle of Provenance Tracing Using Lead Isotopes

Lead has four stable isotopes: ^{206}Pb and ^{207}Pb, whose Natural Abundance (NA—the share of each isotope of an element in a given number of atoms of this element) is about 24.1% and 22.1%. These isotopes are the result of the radioactive decomposition of ^{238}U and ^{235}U respectively, while ^{208}Pb (NA about 52.4%) is being produced by the radioactive decomposition of ^{232}Th. ^{204}Pb (NA is about 1.4%) is not radiogenic and thus occurs in constant abundance since the formation of the Earth. An increase in ^{207}Pb is so slow that it can practically be considered zero (see, *e.g.* Baron *et al.,* 2014: 665–666, 676; Albarède *et al.,* 2020: 3; Pernicka, 2014: 247; see also Albarède *et al.,* 2012: 853–854). Since the Pb isotopes generally do not undergo fractionation (some cases where fractionation may occur are discussed later in the text), Pb isotopic ratios are supposed to be conserved after the ore is smelted into metal (De Ceuster & Degryse, 2020: 108; Artioli *et al.,* 2020: 2; Pernicka, 2014: 248–249; Albarède *et al.,* 2012: 853–854; see also Gale, 2009: 192), although the overall picture can be seriously affected by metal mixing and recycling (see, *e.g.* Ling *et al.,* 2019: 2; Nørgaard *et al.,* 2019: 17; Pernicka, 2014: 248).

It has been proposed that another possible advantage of the use of Pb isotopic ratios in provenance studies may consist in the absence of any significant differences in the isotope abundances between Pb in slag and Pb in the metal (Pernicka, 2014: 249). Based on slag from argentiferous galena ores S. Baron and colleagues generally confirm the usefulness of slag in non-ferrous metal provenance studies, both concerning its Pb isotopic and trace element composition in cases where the slag can be dated to confirm that it is contemporary with the artefact whose origin is being traced (Baron *et al.,* 2014: 670). Slag may also constitute evidence of smelted ores (and possibly mixtures of smelted ores), which may be particularly valuable if

the mined veins are no longer available due to later industrial-scale activities. Therefore, an isotopic match might sometimes indirectly imply provenance, even if the chronology of a given artefact and the archaeological dating of slag are at variance. Indeed, if a significant amount of slag is reported, it can be assumed that it comes from local production and is therefore also characteristic of the signature of local ore deposits. Of course, all other necessary prerequisites to verify a provenance hypothesis must be met in such a case (see below).

Limitations Inherent in Provenance Tracing Using only Lead Isotopes

The use of Pb isotopes for provenance studies is burdened with some major issues. The most well-known problems (which also apply to chemistry-based studies) are different accuracy, precision, and detection limits of analytical instruments or possible contamination introduced by sampling. A general and obvious provenance prerequisite is that within-group variance in possible metal sources must be lower than their between-group variance. However, the Pb isotopic composition of ores is a result of several geological factors, such as the deposit age and time span of deposition, the origin of the mineral, or later geological events. Thus, even a single source is likely to have a broad range of ratios, and the distribution of ratios is not normal in most cases. Later geological events could result in the remobilisation of earlier deposits and create new ore bodies with narrower isotopic composition ranges. Moreover, there is always a chance that geographically distant ore deposits will display similar Pb isotopic ratios. All this means that there may be a strong overlap of isotopic signatures from different regions, and the statistical processing of data is a complex task (Baron *et al.,* 2014: 667–669; De Ceuster & Degryse, 2020: 109; Killick *et al.,* 2020: 87, 89; Artioli *et al.,* 2020: 2; Radivojević *et al.,* 2019: 138; Pernicka, 2014: 250–251, Fig. 11.4; Pollard, 2009: 182–187). Apart from that, the Pb in copper alloys can originate from several sources, such as, *e.g.* tin (De Ceuster & Degryse, 2020: 111; see also Artioli *et al.,* 2020: 16). Yet another problem is posed by the possible mixing of metal from multiple sources, including recycling, or by the smelting of mixed ores (see, *e.g.* Liu *et al.,* 2022; Killick *et al.,* 2020: 89–90, 98; De Ceuster & Degryse, 2020: 108; Nørgaard *et al.,* 2019: 17; Nørgaard *et al.,* 2021: 12–13, 17–19, 24; Pernicka, 2014: 256–259; Liu & Pollard, 2022: 1–2, 4, 7; Bray *et al.,* 2015: 203–204, 208; on possible ore mixing see recently Rademakers *et al.,* 2020: 16). The original isotopic signature can also be blurred by intentional addition of lead to copper. Some scholars assume that a Pb content below 1% almost certainly indicates no intentional Pb addition, while anything above 5% of Pb implies intentional addition. Interpretation of Pb content between 1 and 5% has been a matter of debate (Pernicka, 2014: 255–256; see also Liu & Pollard, 2022: 1–2, 4, 7, 8, Fig. 4). Almost all artefacts discussed in our study contain Pb at levels below 1%, so intentional Pb addition does not seem to be a problem here.

Difficulties may also be caused by possible fractionation, for example in the case of slag. S. Baron and colleagues point to the existence of some differences in the Pb isotopic composition between the metal and the silicate matrix of slag in argentiferous lead ores. They therefore recommend analysing metal prills in slag,

rather than focusing on its silicate matrix, as metal prills can provide information on possible ore mixing and additions to metal in the production process. The Pb isotopic signature of such metal prills may be a more valuable source of information compared to heterogeneous ores, as they provide data on the metal that was produced at a specific place and time (Baron *et al.,* 2014: 670, 671, Table 1, 672, Fig. 2). The problem of fractionation has also been discussed by J. Cui and X. Wu. They have experimentally found out that fractionation can in fact occur. However, they have assumed that alteration of the original Pb isotopic ratios is so small (less than 0.1%) that for most ancient metallurgical processes it will not be an impediment in provenance studies (Cui & Wu, 2011: 206–213).

Other cases of fractionation have been mentioned by F. W. Rademakers and colleagues. Although there was generally a match between ores, slag, and copper Pb isotopic ratios, there were also some differences between ores and slag. Although the examined slags might fit within the range of Pb isotope ratios of ores, they could differ from the individual ore blocks they were smelted from. Some significant changes in Pb isotopic ratios could occur in the smelting process (possible fuel contamination), especially in the case of ores with low Pb content (Rademakers *et al.,* 2020: 11, 12, Fig. 6, 13, 14, Fig. 7, 15-17). These observations are of relevance for our research, as one of the deposit sources discussed in one of our case studies comprises both ore and slag. The latter includes exclusively Pb isotopic ratios as no chemistry data was available.

The usefulness of individual Pb isotopic ratios has been considered. F. Albarède and colleagues say that each of the Pb isotopes can be selected as a denominator in provenance studies, and each of these selections has its advantages and disadvantages (Albarède *et al.,* 2020: 3–6; see also Killick *et al.,* 2020: 87; De Ceuster & Degryse, 2020: 110; Albarède *et al.,* 2012: 854–855). G. Artioli and colleagues recommend applying ^{204}Pb-normalised ratios (^{206}Pb/^{204}Pb, ^{207}Pb/^{204}Pb, ^{208}Pb/^{204}Pb) as these ratios are consistent with geological interpretations and better discriminate between ore bodies (Artioli *et al.,* 2020: 4). S. Baron and colleagues also argue that these ratios have more potential in provenance studies, while ^{207}Pb/^{206}Pb and ^{208}Pb/^{206}Pb plots do not discriminate based on the sources of individual ores and offer no distinction between deposit ages (Baron *et al.,* 2014: 676–677). In this paper, since different Pb isotopic ratios were used by the authors of the case studies we discuss, we have decided to use the values of all four Pb isotopes. This approach is also in line with what S. Baron and colleagues state on the significance of the ^{204}Pb isotope, saying that "archaeological materials can only be derived from ores with which they share the same isotopic space, as defined by all the Pb isotopes" (Baron *et al.,* 2014: 677).

Another issue is posed by the fact that Pb isotopic ratios alone cannot distinguish between ore deposits of the same geological age. What is more, Pb isotopic signatures can provide negative evidence on provenance (*i.e.* they can disprove the origin of metal from a given ore). However, to positively identify provenance from an ore body, it is first necessary to exclude all other possible sources. For this purpose, it is indispensable to also consider data provided by chemistry, geology, geography, and archaeology, including archaeometallurgy (Artioli *et al.,*

2020: 2; Radivojević *et al.,* 2019: 138–139; Pernicka, 2014: 249–250; Baron *et al.,* 2014: 669; see also Athanassov *et al.,* 2020: 329).

Use of Trace Elements in Non-Ferrous Metal Provenance Studies

A proper selection of trace elements for non-ferrous metal provenance studies is also crucial. It is generally assumed that there is some match between the trace element signature in copper and that in the ore it was smelted of (Radivojević *et al.,* 2019: 139). A prerequisite is that the only useful elements are those whose ratio to copper remains similar in all stages of manufacture from ore to final artefact. An obvious problem can be posed by the general heterogeneity of ores chemistry. What is more, the concentration of some trace elements (such as Ni and As) can be affected by smelting conditions. Generally, smelting, melting, and mixing can seriously affect the concentration of trace elements and thus obscure the relationships between artefacts and raw materials. Elements that form volatile compounds (*e.g.* As, Sb, Zn) may be lost during roasting, and some elements can also be removed by possible copper refining (*e.g.* liquation as a means of separating Ag from Cu). Yet, another problem can be posed by the intentional alloying of some elements such as As, Sn, Pb, and Zn to copper. The possible mixing of ores and metal (including scrap recycling) must also be taken into consideration, although the actual significance of this phenomenon may have been different depending on the given region or period. A possible indicator of mixing is a notable homogenisation of metal chemistry, preventing any identification of metal groups. Conversely, a tendency of artefacts to form chemistry-based groups may suggest the absence of mixing (Pernicka, 2014: 249–259; Bray, 2022: 88–94; Bray *et al.,* 2015: 202–206; Radivojević *et al.,* 2019: 138, 144–148, 156–161; Artioli *et al.,* 2020: 2; De Ceuster & Degryse, 2020: 108; Ling *et al.,* 2019: 24–25; Nørgaard *et al.,* 2019: 17; Liu *et al.,* 2022; Wood, 2022: 193–198). These issues have inclined some researchers to assume that, apart from provenance, more attention should be paid to "life cycles" of copper alloy artefacts and to chemistry changes they may undergo when recycled and reused (see, *e.g.* Bray, 2022; Bray *et al.,* 2015). F. W. Rademakers and co-authors have found out that the concentration of some elements (*e.g.* Ni, As, and Sb) was sometimes significantly lower in copper than in ores. Ore-slag comparisons revealed similarities in As and Ni concentrations and differences regarding Sb (Rademakers *et al.,* 2020: 6–9, 10, Fig. 4, 11, 15, 17). Some researchers express reservations concerning the usefulness of trace elements as provenance markers, especially for noble metals that may have undergone cupellation (Albarède *et al.,* 2020: 2; on this issue see also Killick *et al.,* 2020: 91–92, 100–101). In broad terms, Ni, As, Ag, Sb, Bi, and some other elements can be of use (*e.g.* Ling *et al.,* 2019: 18–24; Nørgaard *et al.,* 2019: 8–10; Pernicka, 2014: 242, 253, Table 11.1; Bray *et al.,* 2015: 205; Radivojević *et al.,* 2019: 142). Although it is often not possible to provenance copper-alloy artefacts based on chemistry alone, in some instances, trace elements can be more significant than Pb isotopic ratios in the determination of parent ores for artefacts (Pernicka, 2014: 250; see also Radivojević *et al.,* 2019: 139).

The Use of Multivariate Statistics in Provenance Studies

First Attempts at Provenance Studies Using Advanced Statistical Treatments

This history of provenance studies of non-ferrous archaeological metal using Pb isotopic ratios and chemistry data is more than 60 years old (*e.g.* Pernicka, 2014: 247–261; Pollard *et al.,* 2018: 36–37; Radivojević *et al.,* 2019: 133–167; Artioli *et al.,* 2020: 1–5; Killick *et al.,* 2020: 86–94). Over the past 60 years, several important advances have taken place, concerning analytical methods (*e.g.* Liritzis *et al.,* 2020: 63, 65–66; Niederschlag *et al.,* 2003: 64–67; Killick *et al.,* 2020: 90, 92; Standish et al. 2021), and the use of new variables, such as Sn or Cu isotopes (*e.g.* Brügmann *et al.,* 2018; Berger *et al.,* 2022a: 57–58, 60–68; Berger *et al.,* 2022b; Artioli *et al.,* 2020: 17, 22–23). However, conventional 2D (sometimes 3D) graphs with Pb isotopic ratios and trace element ratios are still the main tool to demonstrate relationships between ore deposits and artefacts and to suggest their provenance areas (*e.g.* Pernicka *et al.,* 2016a; Ling *et al.,* 2019; Chugayev *et al.,* 2020; Mödlinger & Trebsche, 2020; Orfanou *et al.,* 2020; Berger *et al.,* 2022a; Mödlinger *et al.,* 2021; Oudbashi *et al.,* 2021; Aragón *et al.,* 2022; Berger *et al.,* 2022b; Gavranović *et al.,* 2022; Pryce *et al.,* 2022; see also remarks in De Ceuster & Degryse, 2020: 110). Advanced statistical methods can be a valuable addition or alternative to such traditional biplots (Radivojević *et al.,* 2019: 136; Artioli *et al.,* 2020: 3; cf. Killick *et al.,* 2020: 87).

The idea of using multivariate statistics in this field of research is not new. Among the first attempts at chemistry-based grouping of metal finds, there was also multivariate cluster analysis. This analysis allowed for the simultaneous examination of many variables. However, it also posed problems, such as data pre-processing or the number of clusters to be isolated (Pernicka, 1990: 89–99; Pernicka, 2014: 242–246). In the 1980s, B. Ottaway applied cluster analysis and discriminant analysis in studies on the composition of the archaeological metal. M. J. Baxter and colleagues discussed the use of Kernel Kensity Estimates (KDE) (Baxter *et al.,* 1997). S. De Ceuster and P. Degryse applied a KDE-based approach in a series of case studies, including Roman Period lead and silver artefacts. This method was selected because KDE does not assume the normal distribution of data (see below), allows for a visual and mathematical (and thus more robust) assessment of provenance, and accounts for scenarios of possible mixing and recycling (De Ceuster & Degryse, 2020: 110–115; on the KDE applicability see also Pollard, 2009: 186 and Gale, 2009: 191–193, Fig. 1).

At the turn of the twentieth and twenty-first century, another method, PCA (Principal Component Analysis), became widespread in such studies (Pollard *et al.,* 2018: 31–32, Fig. 5, 33). Average linkage cluster analysis was applied by M. Schreiner to analyse the chemistry of Slovak copper ores (Schreiner, 2007: 49–52). This method was also used by Z. Siklósi and M. Szilágyi to examine the chemistry of Hungarian Copper Age artefacts (Siklósi & Szilágyi, 2019: 5280–5281). PCA was applied by C. Canovaro in a study of Bronze Age Alpine copper (Canovaro, 2016: 35–36, 72–73, Fig. 5.2, 74, 78–79, Fig. 5.5, 90–91, Fig. 5.11). PCA on a set of trace

elements has recently been used by T. Birch and colleagues to examine relationships between the trace elements and Pb isotopic patterns in Magna Graecia's silver coins (Birch *et al.,* 2020: 102–104, Fig. 6). The same method was applied by H. W. Nørgaard and co-authors for investigating relationships between types of copper in artefacts (Nørgaard *et al.,* 2019: 15, Fig. 10, 16-17). In another paper, these authors also conducted an average-link cluster analysis to define artefact groups and to propose provenance hypotheses (Nørgaard *et al.,* 2021: 5–6, Fig. 2, 7, Tabs. 2 and 3, 8). Other recent examples of the use of PCA include a study of the chemical composition of Chinese bronzes by J. R. Wood and Y. Liu (Wood & Liu, 2022: 18, Fig, 8, 26–27) and an examination of the chemistry of copper alloy artefacts from Early Iron Age Mongolia (Hsu *et al.,* 2020: 5–6, Fig. 3b).

R. Gebhard and R. Krause examined the famous Early Bronze Age Nebra hoard with a hierarchical cluster analysis (average linkage, squared Euclidian distances) on Pb isotopic ratios. According to these authors, other clustering procedures could also be used, such as the centroid method or Ward's method (Gebhard & Krause, 2020: 331, Fig. 3, 332). The use of such clustering methods was heavily criticised by E. Pernicka and co-authors, due to the lack of the normal distribution of Pb isotopic ratios. Therefore, the proposed conclusions were found untenable (Pernicka *et al.,* 2020: 107, Fig. 21, 108–109). This issue is discussed in detail below.

Hierarchical cluster analysis based on Euclidian distances and Ward's method was used by F. Albarède and co-authors in a study of Roman republican silver coins. Data processing in this analysis also included the kappa-mu (κ-μ) geological age calculations for individual silver ore deposits (Albarède *et al.,* 2020; see also Albarède *et al.,* 2012, with another two case studies). The significance of geological histories of deposits has also been underlined by D. J. Killick and colleagues (Killick *et al.,* 2020: 87, 89; see also Baron *et al.,* 2014: 669) and by J. Milot and co-authors specifically for Pb deposits (Milot *et al.,* 2021). 3D Euclidean distances were also used on Pb isotopic data by several authors to trace the origin of copper alloy artefacts (Canovaro *et al.,* 2019, Artioli *et al.,* 2017 and Stos, 2009).

Recent Studies Coupling PCA and Agglomerative Hierarchical Clustering (AHC)

C. Tomczyk and co-authors discussed a method in which PCA is coupled with AHC. Pb isotopic ratios data ($^{208}P/^{206}Pb$, $^{207}Pb/^{206}Pb$, $^{206}Pb/^{204}Pb$, $^{207}Pb/^{204}Pb/^{208}Pb/^{204}Pb$) is first centred (*i.e.* a mean value for a given variable is subtracted from the value of each observation for this variable) and is then processed by a covariance-type PCA. Next, AHC is run on PC scores using Pearson's correlation coefficient index of similarity and an average linkage agglomeration. Clusters are isolated with automatic maximum inertia truncation. This method removes problems caused by outliers (these can greatly contribute to the lack of normal distribution in Pb isotopic data), which are simply assigned to separate classes (Tomczyk *et al.,* 2021a: 167–171). When tested on case studies, this approach allowed for the successful separation of Alpine copper ores or for a provenance examination of Sardinian and Cypriote ingots (Tomczyk *et al.,* 2021a: 172–174, Figs. 2-4, 175–176, Fig. 5, 178, Fig. 8).

These authors stress that the geological nature of deposits must also be considered (Tomczyk *et al.,* 2021a: 168, 177), which was reiterated in another paper (Tomczyk *et al.,* 2021b: 2–5). They also suggest other possible statistical methods, such as Discriminant Analysis (DA), although it requires several prerequisites, or Multiple Correspondence Analysis (MCA), which can simultaneously handle quantitative (Pb isotopic ratios) and qualitative (geological groups) data (Tomczyk *et al.,* 2021b: 5–6, 9–10). The PCA-AHC approach was re-tested, and it demonstrated a good separation of geological deposit groups from the Italian and the French Alps (Tomczyk *et al.,* 2021b: 6–7, Figs. 2 and 3, 8, Figs. 4 and 5, 9, Figs. 6 and 7). Although the use of five Pb isotopic ratios can be a matter of debate (see Section "Limitations Inherent in Provenance Tracing Using only Lead Isotopes"), these papers convincingly demonstrate the applicability of the method in the field in question. In addition, PCA-AHC treatments on trace elements of copper alloy artefacts were performed by K. Costa and collaborators (Costa *et al.,* 2021).

Some remarks must also be made on recent developments in iron provenance studies. This is mainly because the chemistry of iron ores or smelting-related slag inclusions in iron poses the same problems as the chemistry of non-ferrous metals or their Pb isotopic composition do, that is, the heterogeneity of the data and the lack of normal distribution. Although metal mixing is not an issue for bloomery iron, strong overlaps between chemistries of iron ore bodies can be a serious obstacle (*e.g.* Charlton *et al.,* 2012) as it is for non-ferrous metal ores. Although new perspectives have been opened by studies of Os isotopic ratios (*e.g.* Brauns *et al.,* 2013; Brauns *et al.,* 2020; Schwab *et al.,* 2022; see also Schwab *et al.,* 2006 for an attempt at using Pb isotopic ratios), this method is not widely used yet. Therefore, chemistry-based examinations are still the most common tool. Earlier works used biplots with ratios of major oxides (*e.g.* Buchwald, 2005; Buchwald & Wivel, 1998) or trace elements (*e.g.* Coustures *et al.,* 2003, 2006). M. F. Charlton and colleagues suggested a method where provenance hypotheses were proposed using PCA, Linear Discriminant Analysis (LDA), and KDE (Charlton *et al.,* 2012: 2283–2291). S. Leroy and co-authors discussed relationships between artefacts based on an LDA-AHC approach with major oxides and trace elements (Leroy *et al.,* 2012: 1084, Fig. 2, 1085–1088, 1089, Fig. 7, 1090–1091; see also Leroy *et al.,* 2018: 2145, 2150–2151, Figs. 8-10, 2152–2153, Fig. 12). Cluster analysis and PCA were used by T. Birch and M. Martinón-Torres to identify smelting systems in iron bars (Birch & Martinón-Torres, 2014: 71, 72, 74, Figs. 3 and 4, 75).

A. Disser and co-authors discussed iron provenance by conducting a PCA-AHC analysis on log-ratio values of major and trace elements (Disser *et al.,* 2016a: 154, 155, Fig. 4, 156, 157, Fig. 6). This method was applied in a three-stage form in another paper of these authors, where all details were specified, such as the choice of Ward's method which minimises within-group variance, and the truncation procedure using an "elbow-type method" (Disser *et al.,* 2016b: 499–500, 501, Fig. 1, 502, Fig. 2, 503–504, Fig. 4, 505, Fig. 5; for other studies see, *e.g.* Dillmann *et al.,* 2017, combining elemental and Os isotope analyses). A combination of AHC and DA was applied by A. Jouttijärvi (Jouttijärvi, 2020: 41, Fig. 5, 42, 45, Fig. 10, 46, Fig. 11, 47, Fig. 12, 48), while PCA was used by I. A. Stepanov and colleagues (Stepanov

et al., 2021: 15–19, 20, Fig. 19, 21; see also Bérard *et al*., 2022a). PCA, LDA, and AHC (Ward's method) were used by M. L'Héritier and co-authors (L'Héritier *et al.,* 2020: 9, Fig. 5, 10, Fig. 6, 11, Figs. 7 and 8, 12, Figs. 9 and 10, 13-15). On the other hand, E. Bérard and colleagues preferred a PCA-LDA approach. The choice of LDA was explained by stating that "this method is a supervised classification approach and has been used, in this study, to graphically maximize the separation between the groups" (Bérard *et al.,* 2020: 2588; Bérard *et al.,* 2022b: 90). A detailed discussion on the LDA method can be found in Section "Advantages of the Statistical Treatment, its Possible Limitations and Importance of Input Data".

All these examples suggest the viability of multivariate methods, including PCA-AHC, in metal provenance studies. The possibility of using PCA and LDA for Pb isotopic ratios (on the example of three copper ore fields) was also proposed by M. Baxter, with a sound recommendation to carry out a preliminary data inspection with ratio biplots to select information-carrying variables (Baxter, 2015: 172–173).

Methods—Details of the Statistical Treatment

Step-by-Step Description of the Methodology

In our approach, Pb isotopes are first converted to Natural Abundance (NA). A recent example of separating the Pb isotopic ratios into their individual isotopes can be found in the work of Y. H. Hsu and colleagues. In this case, this was done to plot ^{206}Pb, ^{207}Pb, and ^{208}Pb isotopes on ternary graphs, as it was assumed that the inclusion of all data in a single graph would provide a better comparison between artefacts and sources in provenance studies (Hsu *et al.,* 2020: 4–5, 9–10, 11, Figs. 7-8, 12, 13, Fig. 9a-b). However, in our study, this breakdown into NA has two main aims. Firstly, NA data of all Pb isotopes can be used standalone instead of Pb isotopic ratios as a dataset. PCA-AHC results based on Pb isotopic ratios and using NA values of individual Pb isotopes can be very similar, or sometimes identical. However, the other aim of the breakdown is that NA values allow for an estimation of the percentage of each Pb isotope in the overall Pb concentration in individual observations. It is thus possible to bring Pb isotopic data to the level of weight units (wt% or ppm) and then to couple it with trace element data to produce combined multivariate isotopic-chemistry datasets. The idea of using Pb isotopic data and chemistry data together has also been applied in other studies. In these works, however, Pb crustal ages (calculated based on Pb isotopic ratios) were plotted on the *X* axis, and chemistry data were plotted on the *Y* axis of traditional biplots (for recent examples see, *e.g.* Wood, 2022: 195–196, Fig. 4, 197–198, Fig. 5; Wood *et al.,* 2019: 8–10, 11, Fig. 4, 12-13, Fig. 6, 14–24). Calculations in our study were carried out in XLSTAT Ver. 2021.5.1, and 3D PCA plots were generated using R Ver. 4.1.3, coupled with R-Studio Ver. 1.1.463. On the other hand, it is possible to do all the analyses using other platforms (more advanced users can conduct the entire bulk of calculations in R). All calculation details for each case study can be found in the electronic

supplementary files. In the paper, however, we only refer to them when we address a detailed issue which is tackled in a specific place of these files.

Our research protocol is as follows:

(1) Pb isotopic ratios are converted into NA of individual isotopes. For this purpose, ratios of $^{208}Pb/^{204}Pb$, $^{207}Pb/^{204}Pb$, $^{206}Pb/^{204}Pb$, and $^{204}Pb/^{204}Pb$ (*i.e.* 1) are summed. Then, 100 is divided by the sum, and ^{204}Pb NA is received, according to the following formula:

$$^{204}Pb = 100/\left(^{208}Pb/^{204}PB + {}^{207}Pb/^{204}Pb + {}^{206}Pb/^{204}Pb + {}^{204}Pb/^{204}Pb\right)$$

Next, the remaining NA values are calculated by multiplying relevant ratios by ^{204}Pb NA. If $*/^{206}Pb$ ratios are available (it is often the case that various works use different sets of Pb isotopic ratios), ^{206}Pb NA is first calculated analogously. Missing ratios can be deduced from the available ones, *e.g.*:

$$^{208}Pb/^{206}Pb = \left(^{208}Pb/^{204}Pb\right)/\left(^{206}Pb/^{204}Pb\right)$$

$$^{207}Pb/^{206}Pb = \left(^{207}Pb/^{204}Pb\right)/\left(^{206}Pb/^{204}Pb\right)$$

$$^{208}Pb/^{204}Pb = \left(^{208}Pb/^{206}Pb\right)/\left[1/\left(^{206}Pb/^{204}Pb\right)\right]$$

$$^{207}Pb/^{204}Pb = \left(^{207}Pb/^{206}Pb\right)/\left[1/\left(^{206}Pb/^{204}Pb\right)\right]$$

The conversion into NA values can be illustrated with an example from our Case Study 1 (for details see Electronic Supplement, Case Study 1, Sheet "1.1 Ingots", Verse 4, Columns T-Z). In this case, $*/^{206}Pb$ ratios were given:

$$^{208}Pb/^{206}Pb : 2.0695;{}^{207}Pb/^{206}Pb : 0.8393;{}^{204}Pb/^{206}Pb : 0.05381$$

$$NA^{206}Pb = 100/(2.0695 + 0.8393 + 0.05381 + 1) = 25.23589\%$$

$$NA^{208}Pb = 2.0695 \times 25.23589 = 52.22568\%$$

$$NA^{207}Pb = 0.8393 \times 25.23589 = 21.18048\%$$

$$NA^{204}Pb = 0.05381 \times 25.23589 = 1.35794\%$$

(2) Atomic Mass (AM—the mass of an atom in atomic mass units (amu); 1 amu is 1/12 of one 12C atom's mass) of individual Pb isotopes in a given composition is calculated by multiplying their NAs in this composition by the atomic mass of each isotope (^{208}Pb amu = 207.9766521; ^{207}Pb amu = 206.9758969; ^{206}Pb amu = 205.9744653; ^{204}Pb amu = 203.9730436):

$$^{204}Pb\ AM = NA^{204}Pb \times {}^{204}Pb\ amu$$

$^{206}\text{Pb AM} = \text{NA}^{206}\text{Pb} \times {}^{206}\text{Pb amu}$

$^{207}\text{Pb AM} = \text{NA}^{207}\text{Pb} \times {}^{207}\text{Pb amu}$

$^{208}\text{Pb AM} = \text{NA}^{208}\text{Pb} \times {}^{208}\text{Pb amu}$

Then, all results are normalised to 100%, *i.e.* ^{208}Pb AM% = ^{208}Pb AM/sum(^{208}Pb AM, ^{207}Pb AM, ^{206}Pb AM, ^{204}Pb AM) × 100, and so on. This step is explained by the following example from our Case Study 1 (for details see Electronic Supplement, Case Study 1, Sheet "1.1 Ingots", Verse 4, Columns AA-AH):

$^{208}\text{Pb AM} = 207.9766521 \times 52.22568 = 10861.722$

$^{207}\text{Pb AM} = 206.9758969 \times 21.18048 = 4383.850$

$^{206}\text{Pb AM} = 205.9744653 \times 25.23589 = 5197.949$

$^{204}\text{Pb AM} = 203.9730436 \times 1.35794 = 276.984$

Normalisation to 100%

$$^{208}\text{Pb AM\%} = 10861.722/(10861.722 + 4383.850 + 5197.949 + 276.984) \times 100 = 52.42016\%$$

$$^{207}\text{Pb AM\%} = 4383.850/(10861.722 + 4383.850 + 5197.949 + 276.984) \times 100 = 21.15706\%$$

$$^{206}\text{Pb AM\%} = 5197.949/(10861.722 + 4383.850 + 5197.949 + 276.984) \times 100 = 25.08602\%$$

$$^{204}\text{Pb AM\%} = 276.984/(10861.722 + 4383.850 + 5197.949 + 276.984) \times 100 = 1.33676\%$$

(3) Wt% or ppm of each isotope in relation to the total Pb content in a given observation is calculated, *i.e.* ^{208}Pb wt% = ^{208}Pb AM% × (Pb wt%/100) and so on. The wt% sum of all Pb isotopes should be equal to the total Pb wt%. This stage is illustrated by an example from our Case Study 1 (for details see Electronic Supplement, Case Study 1, Sheet "1.1 Ingots", Verse 4, Columns AI-AN):

Pb ppm: 25

$^{208}\text{Pb ppm} = 52.42016 \times 0.25 = 13.10504$

$^{207}\text{Pb ppm} = 21.15706 \times 0.25 = 5.28927$

$^{206}\text{Pb ppm} = 25.08602 \times 0.25 = 6.27150$

$^{204}\text{Pb ppm} = 1.33676 \times 0.25 = 0.33419$

(4) Variable sets are prepared. These can include Pb isotopic data alone, combined Pb isotopic and chemistry data, or chemistry data only. The need to produce multiple variable sets results first from the low number of available datasets with complete Pb isotopic and chemistry data for all observations. This is especially true for ore deposits, where chemistry data is missing or such information is available for only a minority of observations (Radivojević *et al.,* 2019: 139; Baron *et al.,* 2014: 669; Prof. Zofia Stos-Gale, Prof. Gilberto Artioli, personal communication). Therefore, in most cases, it will be possible to employ variable sets with Pb isotopic data only, until more complete Pb isotopic-chemistry datasets become available. On the other hand, in some instances, combined variable sets can be applied, and for some purposes, researchers can focus solely on chemistry issues. The selection of variables in each set can be decided upon individually, as presented in the discussion on the usefulness of individual Pb isotopic ratios and trace elements (see above). However, to compare results, we have decided to use the same variables (with the reservation that Pb isotopic ratios are replaced with values of individual isotopes) as the authors of our case studies did.

These variable sets are compositional data, *i.e.* their values sum up to a constant unit. In this case, it is 100, be it 100% of NA of all isotopes or wt% of all isotopes and/or trace elements (if normalised to 100%). Therefore, data transformation is necessary to provide all variables with a similar weight. Otherwise, PCA results will be dominated by variables with the largest variance (or the highest spread of values). Out of several choices (Charlton *et al.,* 2012: 2283–2284; Baxter, 2015: 106–111; Żabiński *et al.,* 2020: 4, with its Electronic Supplement: 21–22; Wood & Liu, 2022: 6, 15; Hsu *et al.,* 2020: 10), we have used a variant of the log-ratio transformation, namely, the centred log-ratio (clr). It centres the transformed variables around 0, and it is expressed by the following formula:

$$y = \log\left[\frac{x}{g(x_1 \cdots x_N)}\right]$$

y - transformed value
x - the value of the variable in a given observation
$g(x_1 \ldots x_N)$ - geometric mean of individual variables in a given observation

Variable Set 1 includes NA values of Pb isotopes. Wt% values could also be used, but when such a dataset is processed by PCA, 100% of the variability is shown on the PC1 axis. The graph therefore becomes "flat" and not very useful. Individual NA values are rescaled to 0–1 (and not log-ratio transformed, for the same reason), using the formula:

Table 1 Comparison of centred log-ratio values of data not normalised to 100% and normalised to 100%

Data not normalised to 100%							
^{208}Pb (%)	^{207}Pb (%)	^{206}Pb (%)	^{204}Pb (%)	Ni (%)	Ag (%)	Sb (%)	As (%)
0.02624	0.01062	0.01246	0.00067	0.04	1.42	2.15	1.71
Centred log-ratio values							
^{208}Pb	^{207}Pb	^{206}Pb	^{204}Pb	Ni	Ag	Sb	As
−0.4167	−0.8095	−0.7400	−2.0107	−0.2337	1.3166	1.4967	1.3973
Data normalised to 100%							
^{208}Pb (%)	^{207}Pb (%)	^{206}Pb (%)	^{204}Pb (%)	Ni (%)	Ag (%)	Sb (%)	As (%)
0.4887	0.1978	0.23211	0.01245	0.7449	26.443	40.037	31.844
Centred log-ratio values							
^{208}Pb	^{207}Pb	^{206}Pb	^{204}Pb	Ni	Ag	Sb	As
−0.4167	−0.8095	−0.7400	−2.0107	−0.2337	1.3166	1.4967	1.3973

$$y = \frac{x - \min(x)}{\max(x) - \min(x)}$$

y - rescaled value
x - the value of a given variable
min(x) - minimum value of this variable in the dataset
max(x) - maximum value of this variable in the dataset

Variable Set 2 are weight unit values of Pb isotopes and selected trace elements (not normalised to 100%). The normalisation is not necessary here, as the centred log-ratio transformation both on normalised and not normalised data yields identical results. This can be illustrated in Table 1 with an example from our Case Study 2 (for calculation details see Electronic Supplement, Case Study 2, Sheet "Normalisation to 100%").

Observations below the limit of detection or those with 0 values are replaced with the lowest value for a given variable (Baxter & Hancock, 2018: 7; Charlton *et al.,* 2012: 2281). Variable Set 3, used in order to focus solely on chemistry issues, are trace elements only, after the centred log-ratio transformation.

(5) Variable sets are processed using covariance-type PCA, and preliminary conclusions are drawn based on PCA graphs. Then, AHC (dissimilarity type, Euclidian distance, Ward's method of agglomeration) is conducted on PC scores. The reason for clustering is that if no clustering is used, we end up with PC graphs only. While these can also be informative, their interpretative value is highly dependent on the amount of information (*i.e.* % of variability within the studied assemblage) they contain (this is explained in detail in Case Study 3). Furthermore, even if a graph with 100% variability on PC1 and PC2 axes is obtained, our interpretations regarding, *e.g.* individual artefact observations and their relationships to ore deposits, will inevitably be biased by potential human error. Therefore, clustering methods can help remove this ambiguity. Although different clustering methods have been used with good results in previous studies (*e.g.* average linkage in Charlton *et al.,* 2012 or in Tomczyk *et al.,* 2021a), Ward's method was found to be especially robust in minimising the within-group variance and maximising the between-group

variance (Disser *et al.,* 2016b: 499; see also L'Héritier *et al.,* 2020; Albarède *et al.,* 2020). Automatic maximum inertia truncation is conducted and repeated manually if necessary (Charlton *et al.,* 2012: 2284; Disser *et al.,* 2016b: 499). We truncate the dendrogram at the level where the agglomeration rate sharply decreases, which can also be seen in the elbow-like bend of the AHC levels bar chart (hence the method's name). Truncation results (*i.e.* the number and composition of clusters) are compared with PCA graphs.

(6) Eventually, we compare and contrast our results with what is proposed in relevant studies concerning relationships between artefacts, ore deposits, and possible provenance patterns.

Advantages of the Statistical Treatment, its Possible Limitations and Importance of Input Data

E. Pernicka and co-authors state that the lack of normal distribution of Pb isotopic ratios can pose problems with some multivariate approaches. As mentioned, clustering methods applied by R. Gebhard and R. Krause (Gebhard & Krause, 2020) were strongly criticised by E. Pernicka and colleagues for this reason. These scholars say that hierarchical clustering methods could not identify "very elongated groups, because they search for multivariate globular groups, implicitly assuming a normal distribution of the values in each variable. However, lead isotope ratios are usually not normally distributed" (Pernicka *et al.,* 2020: 108, with a reference to Baxter, 1999; see also De Ceuster & Degryse, 2020: 109–110; Gale, 2009: 192, recommends using simple biplots). Although log-ratio is not strictly a data normalisation method (Baxter, 2015: 107, note 2), logarithm transformation is often used as "quasi-standardisation" to reduce the effects of different magnitudes of individual chemical elements and bring them to a similar scale (Glascock, 2016: 8). Remarkably, R. Gebhard and R. Krause did not state whether their Pb isotopic data had undergone any transformation prior to the analysis (Gebhard & Krause, 2020). For the sake of normality comparison between the raw and transformed Pb isotopic data, we have carried out normality tests (Shapiro–Wilk, Anderson–Darling, Liliefors, Jarque–Bera) on data from our Case Study 2. These were four isotopic ratios ($^{208}Pb/^{206}Pb$, $^{207}Pb/^{206}Pb$, $^{206}Pb/^{204}Pb$, $^{204}Pb/^{206}Pb$—raw), as well as centred log-ratio values of Pb isotope NAs (transformed). The result for the Pb isotopic ratios was "not normal distribution" in all 16 cases (*i.e.* four tests for each of the four ratios). However, in the case of the centred log-ratio values, a "normal distribution" result was obtained in four cases. Moreover, normal probability plots (Q-Q plots and P-P plots) clearly demonstrate that the transformed data distribution is much closer to normal (for details see Electronic Supplement, Case Study 2, Sheets "Normality Tests Pb Ratios" and "Normality Tests Pb CLR"). We therefore assume that this reservation raised by E. Pernicka and colleagues is not a major obstacle, provided that proper data transformation is applied.

The lack of normal distribution in the chemistry of non-ferrous archaeological metal has recently been evocated by P. Bray. The absence of data normality would render clustering analyses irrelevant in this field. P. Bray thus quoted the opinion of

other scholars, who explicitly stated that "simple graphical visualisations of chemical distributions" would prove more useful than advanced statistics (Bray, 2022: 90–91). The lack of normal distribution in most cases also applies to the chemistry of iron smelting slag or the chemistry of archaeological artefacts in general (*e.g.* Charlton *et al.,* 2012: 2284; Glascock, 2016: 8). This, however, was not considered an obstacle against the use of the cluster analysis on logarithmic concentrations (*i.e.* transformed data) of trace elements in copper artefacts in the aforementioned study by H. W. Nørgaard and colleagues (Nørgaard *et al.,* 2021). Moreover, the PCA-AHC was routinely applied in the aforementioned provenance studies on iron artefacts, where the lack of normal distribution of chemistry data is commonplace. To examine the distribution of raw and transformed chemistry data, we have carried out four normality tests on four diagnostic chemical elements (Ni, Ag, Sb, As) from Case Study 2, analogous to what has been done on Pb isotopic data. Concerning the raw data, it was only for Ni that two tests suggested a normal distribution, while in the remaining cases, a lack of normality was found. Regarding the transformed data, normality was suggested for Ag by two tests and by one test for As and Sb. As in the case of Pb isotopic data, normal probability plots (Q-Q plots and P-P plots) point out a strong shift toward data normality (for details see Electronic Supplement, Case Study 2, Sheets "Normality Tests Chemistry Raw" and "Normality Tests Chemistry CLR"). We thus believe that the non-normal distribution problem in chemistry data can also be successfully dealt with.

In addition, it is worth noting how the PCA-AHC approach treats the aforementioned "elongated groups", often seen in ore bodies, both with regard to their Pb isotopic composition and their chemistry. This method splits such data into separate classes. Therefore, any overlapping zones or outlying observations of multiple ore bodies will be treated as such distinct units. This is a major advantage of the PCA-AHC over Discriminant Analysis and other "supervised" methods, that is, those which also use the information on the group to which a given observation belongs (in this case, a deposit group). When analysing relationships between possible source bodies (so-called "training sets") for artefacts under consideration, "supervised" methods produce a so-called "confusion matrix", which indicates how observations in individual deposits separate or overlap. If a deposit observation comes from an overlapping zone (which is inevitable for Pb isotopic data in many cases, especially with large datasets), it is assigned to the "confusion area" (examples of such "confusion matrices" can be found, *e.g.* in Żabiński *et al.,* 2020: 8, Table 4, 13, Table 5). Although artefact observations whose compositions are identical or very similar to compositions of overlapping deposit observations will be eventually classified by "supervised" methods to an ore body, the probability of such classifications will be low. On the other hand, PCA and AHC are "unsupervised" methods, *i.e.* no information on the group is used. Therefore, artefacts which are possibly made of mixed metal will go into the aforementioned separate classes (this is shown in our Case Study 3). This is because DA and other "supervised" methods will assign artefact observations only to already existing deposit groups, while PCA-AHC will form new independent classes solely based on the composition of individual observations.

Furthermore, as the NA of ^{204}Pb is low, it could be supposed that its variability would be low, too, and thus its discriminating power would not be very high, either.

To verify this, the NA variability of all four Pb isotopes was examined using the boxplot method, based on data from our Case Study 1. As it can be seen, the variability of NA ^{204}Pb considerably differs in individual bodies of observation. This variability and thus the discriminating power of individual variables is always relative and depends on what bodies of observations we focus on. Therefore, it differs when we divide the observations into "locations" (find places) or into "groups" (artefact type and find place combined) (see Electronic Supplement, Case Study 1, Sheets "Boxplots NA Location" and "Boxplots NA Group").

Eventually, a caveat must be made here. As stated above, the number of datasets with complete Pb isotopic and chemistry data for all observations is still low. Therefore, we only attempted at examining possible artefact-deposit relationships in Case Studies 3, 4, 5 and solely based on Pb isotopic NA values. Furthermore, it is not our aim to propose any new artefact provenance hypotheses. This would require taking new deposits into consideration (a task gravely impeded by the aforementioned data incompleteness), possibly a new discussion on the selection of variables with the highest discriminating power, and is therefore beyond the scope of our paper. Instead, what we intend to do is to verify the proposed method.

Results and Discussion

As mentioned above, we verify our method using a series of literature-based case studies to compare our results with those offered in relevant studies on the basis of the biplot method. We have decided to use these datasets for yet another reason. Namely, they offer a good opportunity (especially Case Studies 3, 4, 5) to examine how the proposed method will treat elongated ore bodies data, how it is able to demonstrate chronology-related differences in Pb isotopic and chemistry patterns in artefacts (Case Study 2), and how it handles observations concerning artefacts that were possibly manufactured of mixed metal (Case Study 3).

Case Study 1—Ingots from Nuragic Sardinia

Among data for copper alloy finds from Bronze Age Nuragic Sardinia, there are 42 ingots from the Bonnanaro, Ittireddu, and Pattada hoards (Begemann *et al.,* 2001: 47–49, 52–53, Table 1, 54–55, Table 2; for a more recent discussion on these finds see Pollard & Bray, 2015). These ingots are generally made of rather pure copper with quite constant trace element patterns and no prominent differences in the chemistry of ingot types. However, some exceptions can be found, such as Ittireddu 62405 or Ittireddu 62417 (Begemann *et al.,* 2001: 50–51, 55) (Fig. 1). Atypical chemistries are followed by atypical Pb isotopic ratios. Apart from these two Ittireddu ingots, this pattern holds for four Bonnanaro finds (SAS-708, SAS-709, SAS-10710, SAS-10711). In terms of their Pb isotopic ratios, most ingots form one main group, Ittireddu 62395 and 62414 being its extension. There are the following exceptions: Ittireddu 62405 and 62417, Bonnanaro SAS-708, SAS-709, SAS-10710, SAS-10711, and at least three

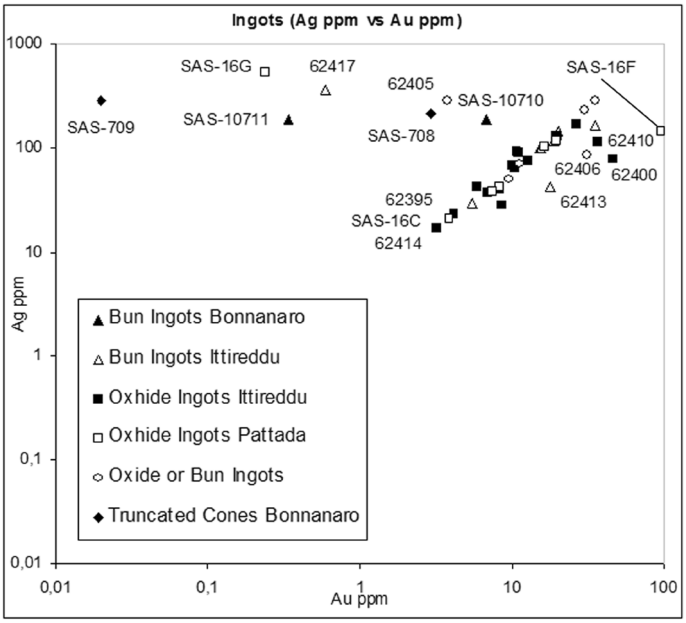

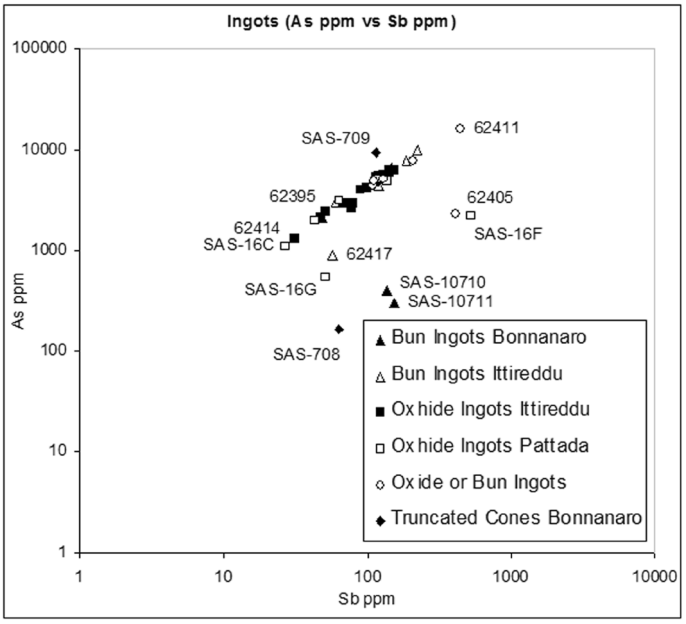

Fig. 1 Ratios of selected trace elements in Sardinian ingots (cf. Begemann *et al.,* 2001: 56, Fig. 7ab). Observation labels were added where possible

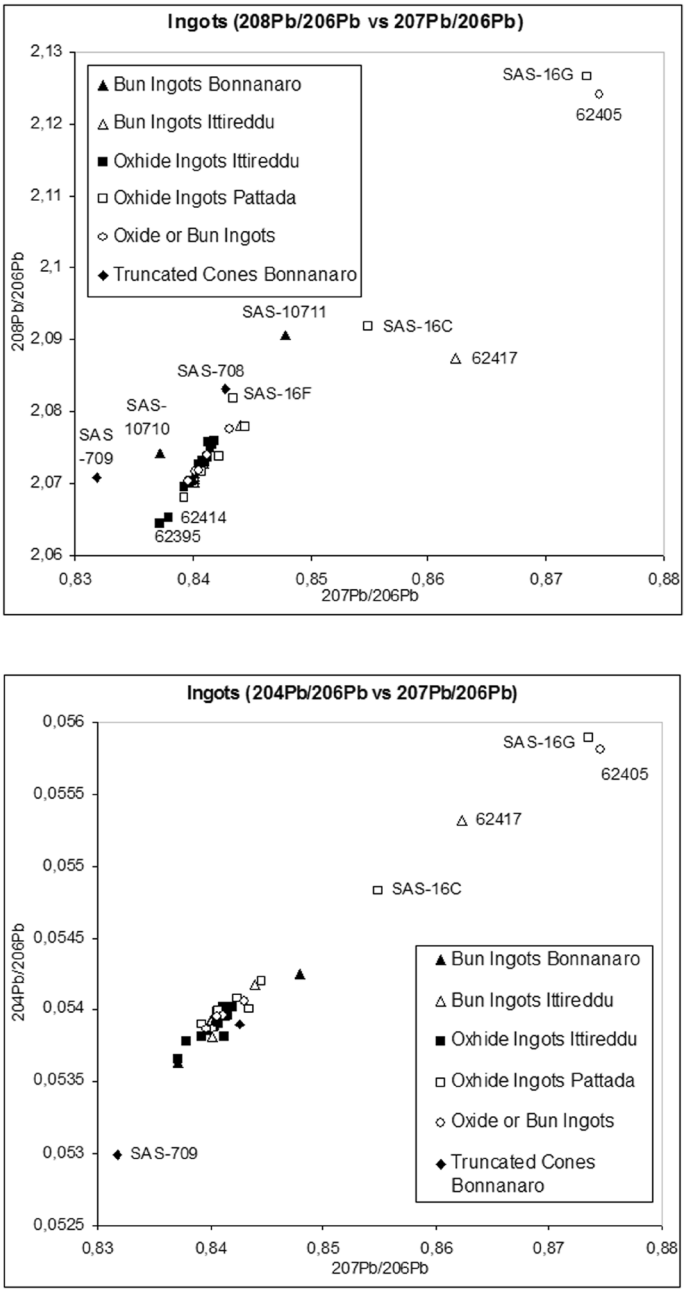

Fig. 2 Pb isotopic ratios of Sardinian ingots (cf. Begemann *et al.,* 2001: 57, Fig. 8). Observation labels were added where possible

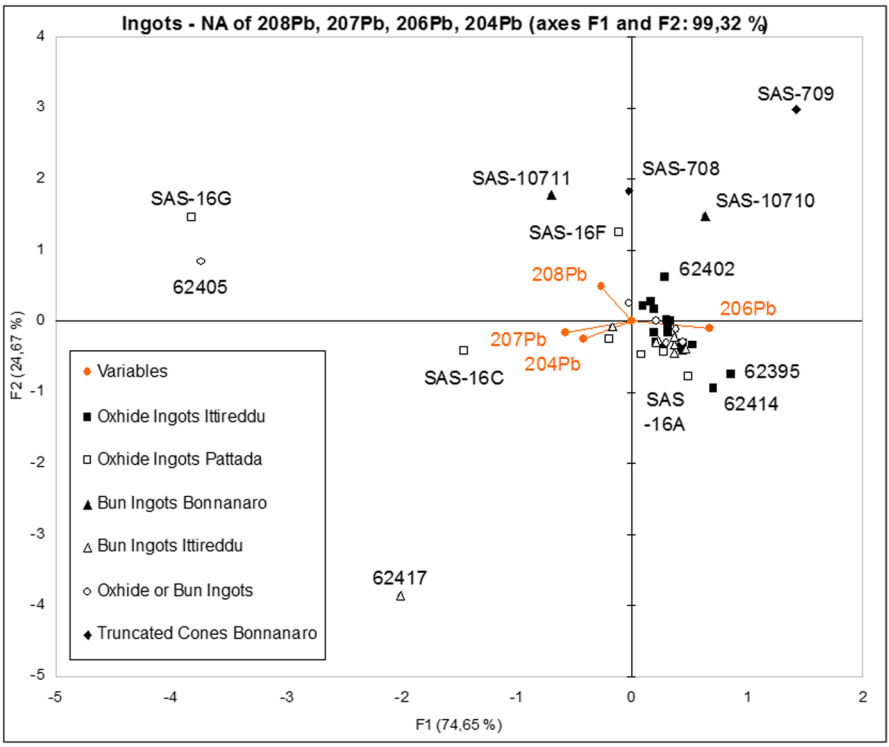

Fig. 3 Sardinian ingots—PCA graph with NA of ^{208}Pb, ^{207}Pb, ^{206}Pb, and ^{204}Pb (0–1 rescaled)

from Pattada [*SAS-16F, SAS-16C, and SAS-16G—C.T. & G.Ż.*] (Begemann *et al.,* 2001: 55, 56, Fig. 7, 57, Fig. 8, 58, Fig. 9) (Fig. 2).

In the next step, we examine whether our method confirms this pattern. This is first done using Variable Set 1. As it can be seen in Fig. 3, there is a good agreement with what F. Begemann and co-authors propose. Most observations form one group near the graph's centre, and Ittireddu 62395 and 62414 can be considered an extension of this cluster. What falls beyond this group are Ittireddu 62405 and 62417, Bonnanaro SAS-708, SAS-709, SAS-10710, and SAS-10711, as well as Pattada SAS-16F, SAS-16C, and SAS-16G. This is also confirmed by the AHC, which isolates four classes (Fig. 4): Class 1—the main cluster; Class 2—Pattada SAS-16C and Ittireddu 62417; Class 3—Pattada SAS-16F, Bonnanaro SAS-10710, SAS-10711, SAS-708, and SAS-709; and Class 4—Pattada SAS-16G and Ittireddu 62405. It is also worth noting that the total variability of the analysed assemblage on PC1 and PC2 axes is 99.32%. In other words, the graph displays almost all information on similarities and differences between the artefacts and is therefore directly readable and interpretable.

These results are verifiable when both Pb isotopes and selected trace elements (Au, Ag, Sb, and As) are considered together (Variable Set 2). As shown in Fig. 5 (which displays 94.75% of the total variability), most observations again form the main group. However, there are observations which were previously classified

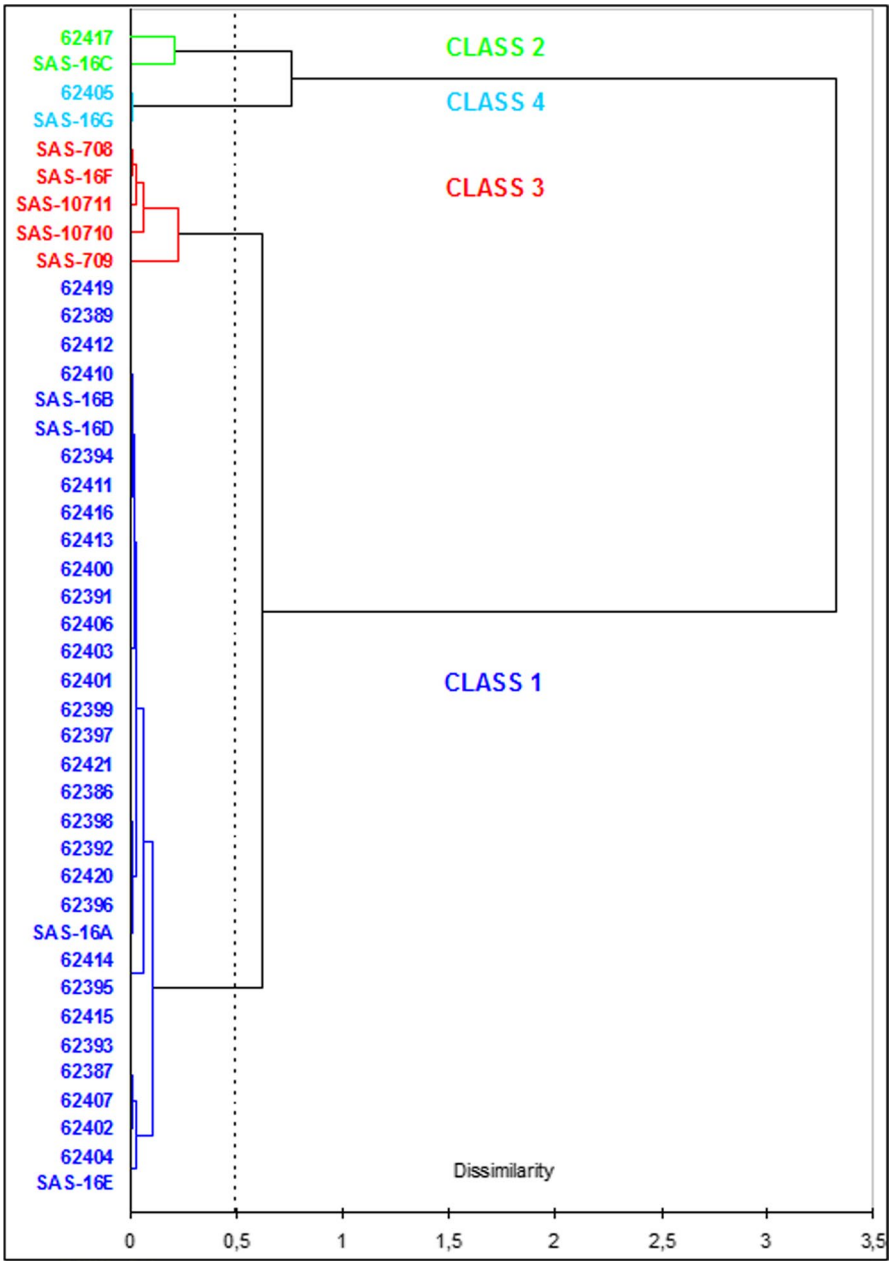

Fig. 4 Sardinian ingots—AHC dendrogram on PC scores with NA of ^{208}Pb, ^{207}Pb, ^{206}Pb, and ^{204}Pb (0–1 rescaled). Level 0.5 truncation

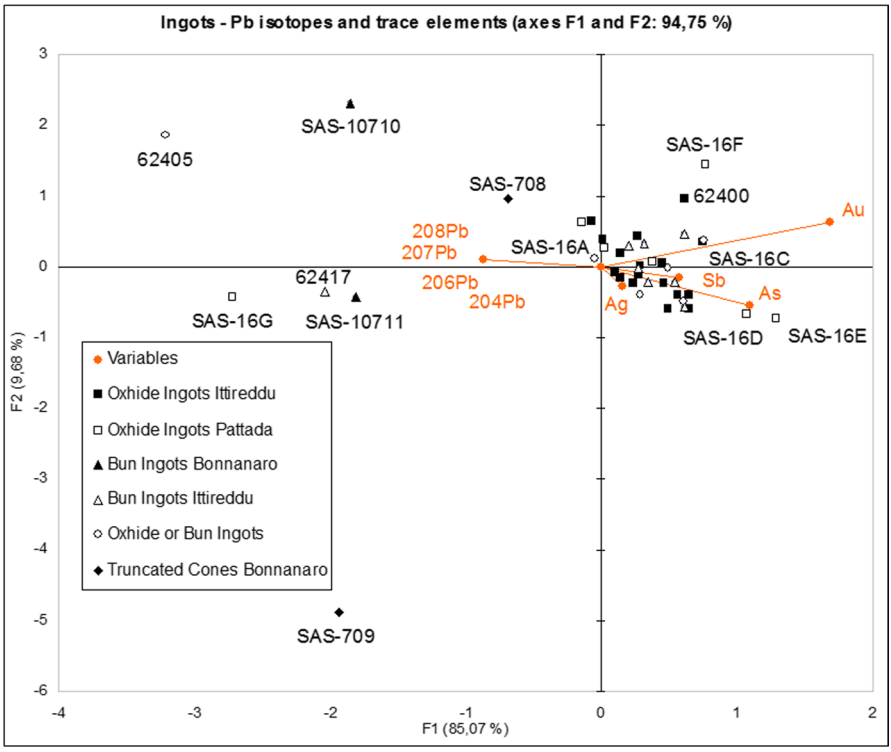

Fig. 5 Sardinian ingots—PCA graph with ppm values of ^{208}Pb, ^{207}Pb, ^{206}Pb, ^{204}Pb, Au, Ag, Sb, and As (centred log-ratio transformed)

outside it solely based on their Pb isotopic fingerprints (Pattada SAS-16C, SAS-16F, and Bonnanaro SAS-708). If their chemistry is also considered, they are within or closer to the main group. This image is confirmed by the AHC, which isolates three classes (Fig. 6). Class 1 encompasses most of the observations, including the three aforementioned ones (SAS-16C, SAS-16F, and SAS-708). Class 2 is formed by Pattada SAS-16G, Bonnanaro SAS-10710, SAS-10711, and Ittireddu 62417 and 62405. Class 3 is solely Bonnanaro SAS-709.

These differences can be explained by the chemistry of these three finds (Fig. 1). Pattada SAS-16C seems to belong to the main group concerning both Au/Ag and Sb/As ratios, while Pattada SAS-16F is within or close to the main group trend field with regard to the Au/Ag ratio (cf. Begemann *et al.,* 2001: 56, Fig. 7a—it is close to the field border in the top-right part of the graph). On the other hand, such a classification of Bonnanaro SAS-708 is potentially caused by this observation being above the Au/Ag main trend field and below the Sb/As trend fields (cf. Begemann *et al.,* 2001: 56, Fig. 7ab). The PCA-AHC approach with Variable Set 2 was able to successfully illustrate relationships between the discussed ingots, except for SAS-708. For this reason, in this case, it would be better to focus on

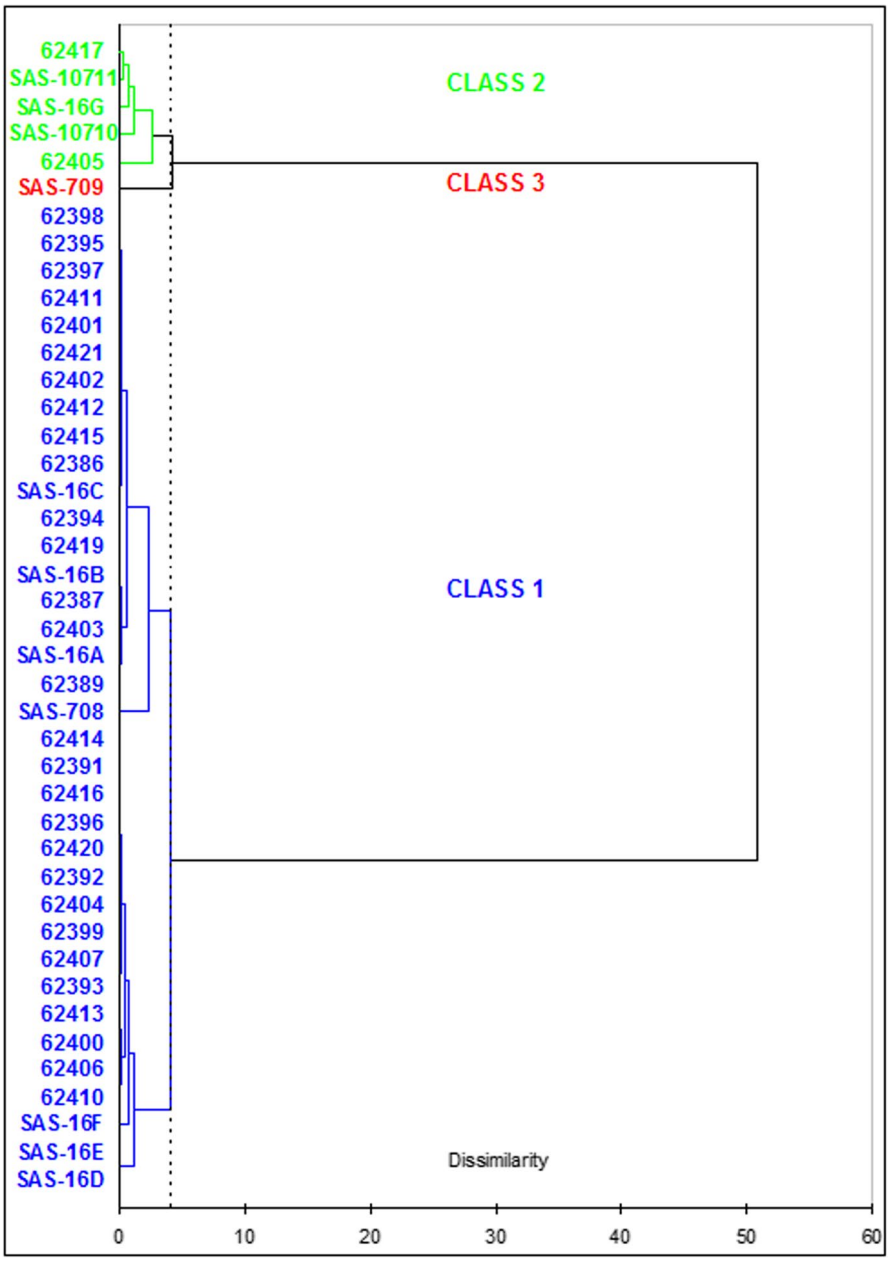

Fig. 6 Sardinian ingots—AHC dendrogram on PC scores with ppm values of ^{208}Pb, ^{207}Pb, ^{206}Pb, ^{204}Pb, Au, Ag, Sb, and As (centred log-ratio transformed). Automatic maximum inertia truncation

the Pb isotopic and chemical compositions of the artefacts in question separately, using Variable Sets 1 and 3.

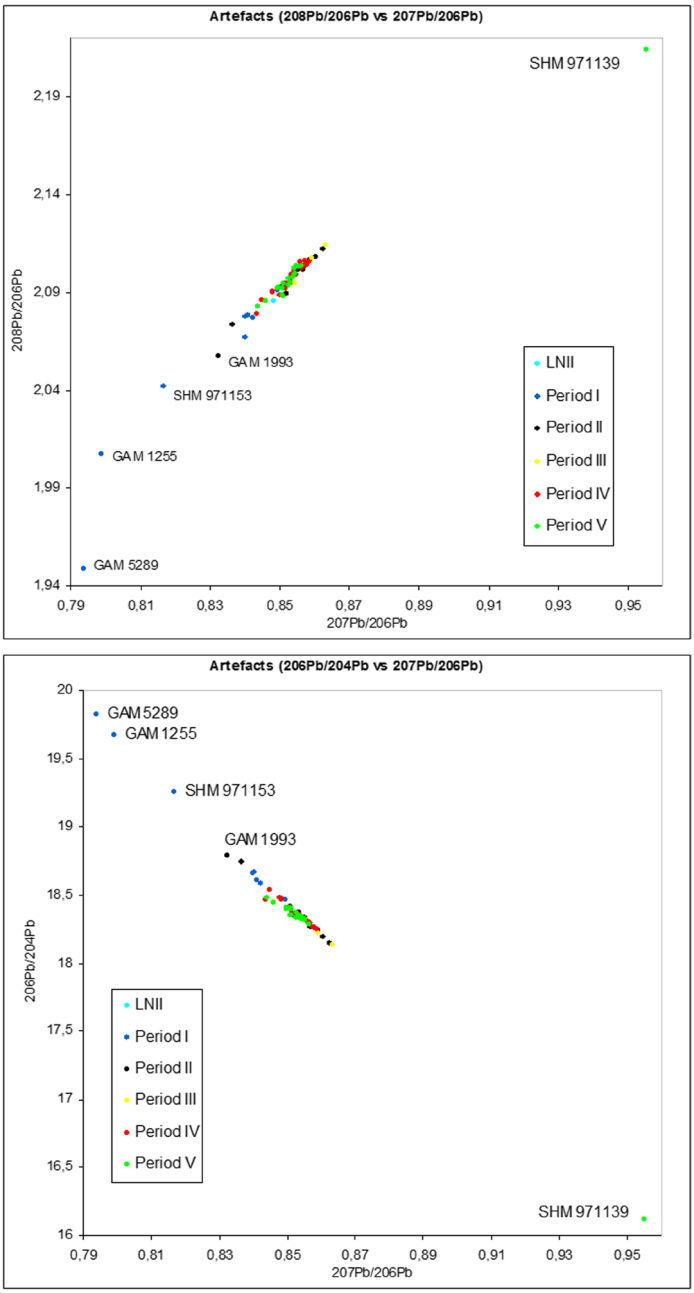

Fig. 7 Pb isotopic ratios of Bronze Age finds from Sweden (cf. Ling *et al.,* 2014: 116, Fig. 9). Observation labels were added to the outlying observations

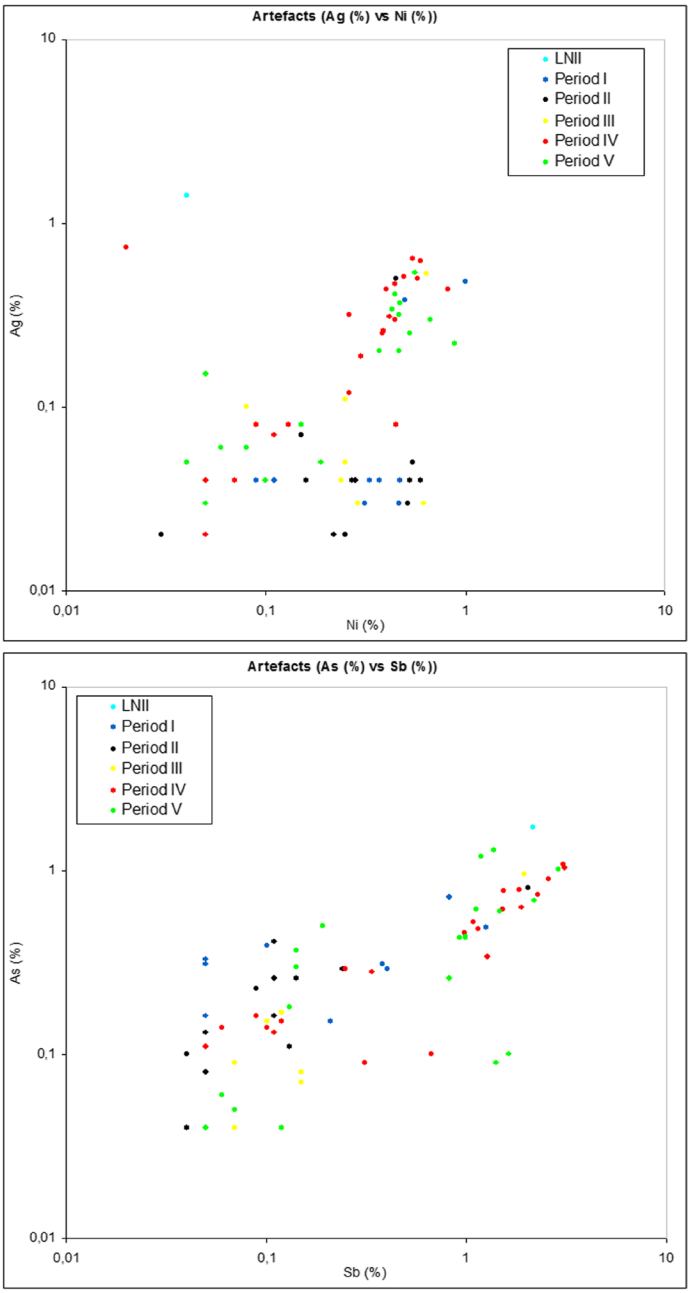

Fig. 8 Ratios of selected trace elements in Bronze Age finds from Sweden (cf. Ling *et al.,* 2014: 121, Fig. 11)

Case Study 2—Bronze Age finds from Sweden

This case includes 71 finds from the Late Neolithic Period II and Bronze Age Periods I–V (2000–700 cal. BC) from Sweden (Ling *et al.,* 2014: 106–108, 109–112, Table 1, 118–119, Table 2, 120–121, Table 3). This study was criticised with regard to some hypotheses concerning metal distribution and artefact provenance, due to a limited comparative database that was used and because of certain interpretation errors (see, *e.g.* Artioli *et al.,* 2020: 2; Athanassov *et al.,* 2020: 326–330; Ling *et al.,* 2019: 26–27; Nørgaard *et al.,* 2019: 15; Bray, 2022: 91). However, in our discussion, we will focus on chronology-related differences in Pb isotopic ratios and chemistry of the finds in question, rather than on their provenance in relation to ores. J. Ling and colleagues say that concerning the Pb isotopic ratios of the finds (Fig. 7), those from different periods form groups related to the extent of individual ore deposits. Furthermore, the finds from later periods (III–IV) are remarkable for their higher $^{207}Pb/^{206}Pb$ vs $^{208}Pb/^{206}Pb$ ratios. A piece of Period V copper slag (Botkyrka SHM 971139) and three Period I axes (Gamleby SHM 971153, Frändefors GAM 1255, Ödsmål GAM 5289) are outliers (Ling *et al.,* 2014: 116, Fig. 9, 117, 119). The content of individual trace elements (As, Sb,

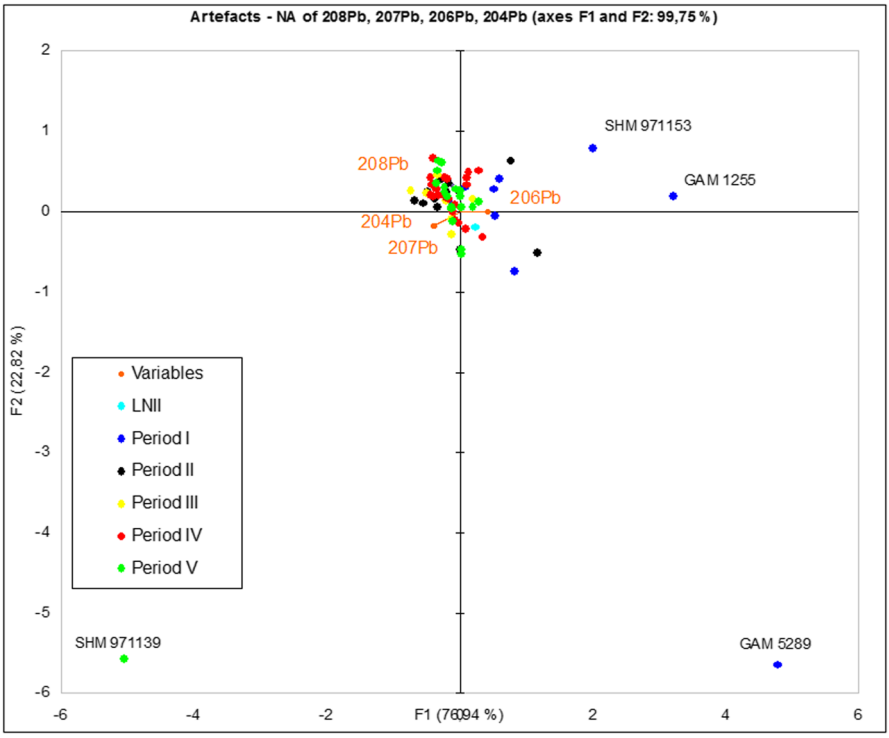

Fig. 9 Bronze Age finds from Sweden—PCA graph with NA of ^{208}Pb, ^{207}Pb, ^{206}Pb, and ^{204}Pb (0–1 rescaled)

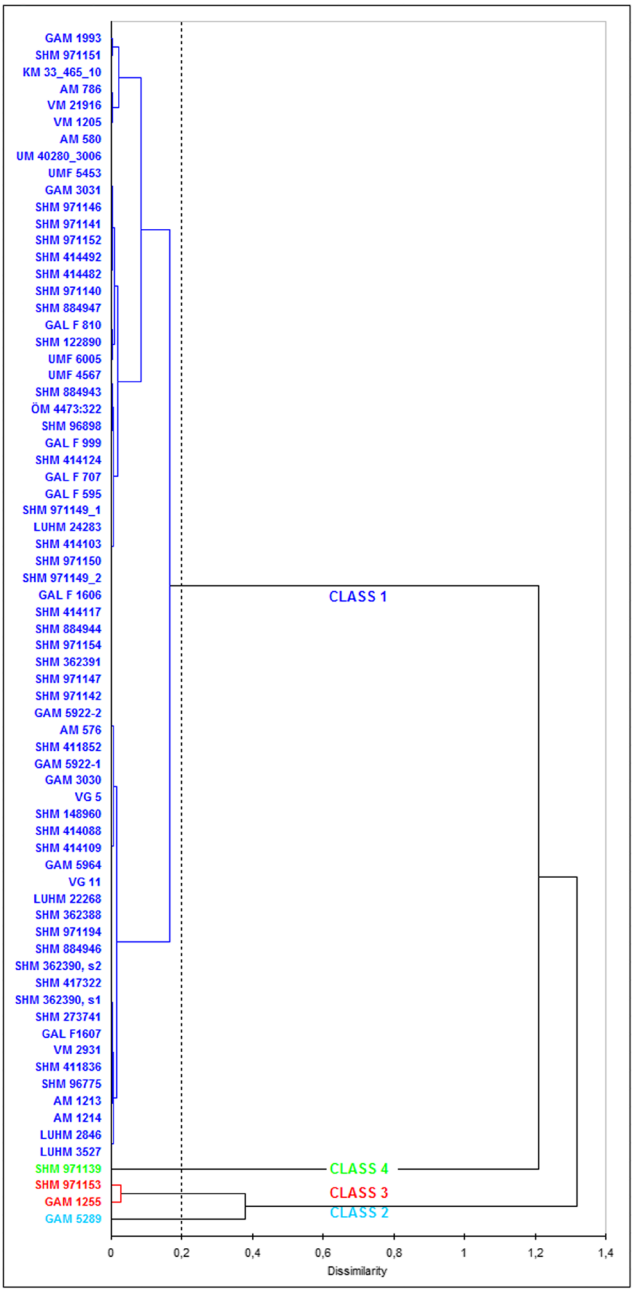

Fig. 10 Bronze Age finds from Sweden—AHC dendrogram on PC scores with NA of ^{208}Pb, ^{207}Pb, ^{206}Pb, and ^{204}Pb (0–1 rescaled). Level 0.2 truncation

Ag, and Ni) in the artefacts is high and varied (Fig. 8), due to different ore geochemistry. A Late Neolithic dagger (Ör SHM 884943) is rich in Sb, As, and Ag, while the finds from Period I are remarkable for lower concentrations of the trace elements than the finds from Periods IV–V. The contents of Sb and Ag in Periods II and III finds are lower as compared with those from earlier and later periods. A majority of the finds from Periods IV and V demonstrate high contents of As, Sb, Ni, and Ag (Ling *et al.,* 2014: 119, 122, Fig. 11).

It can be now examined whether the PCA-AHC method confirms these results. As it can be seen based on Variable Set 1, most observations in Fig. 9 (99.75% of the total variability) cluster near the centre of the PC graph, while the slag from Botkyrka SHM 971139 and the axes from Gamleby SHM 971153, Frändefors GAM 1255, and Ödsmål GAM 5289 are plotted away from it. This is also demonstrated by the AHC results (Fig. 10), where four classes were isolated: Class 1 (main), Class 2 (GAM 5289), Class 3 (GAM 1255 and SHM 971153), and Class 4 (SHM 971139). The manual truncation of the dendrogram is in line with what the PC graph suggests, where GAM 1255 and SHM 971153 seem to form one class, while the two remaining outliers are obviously separate ones.

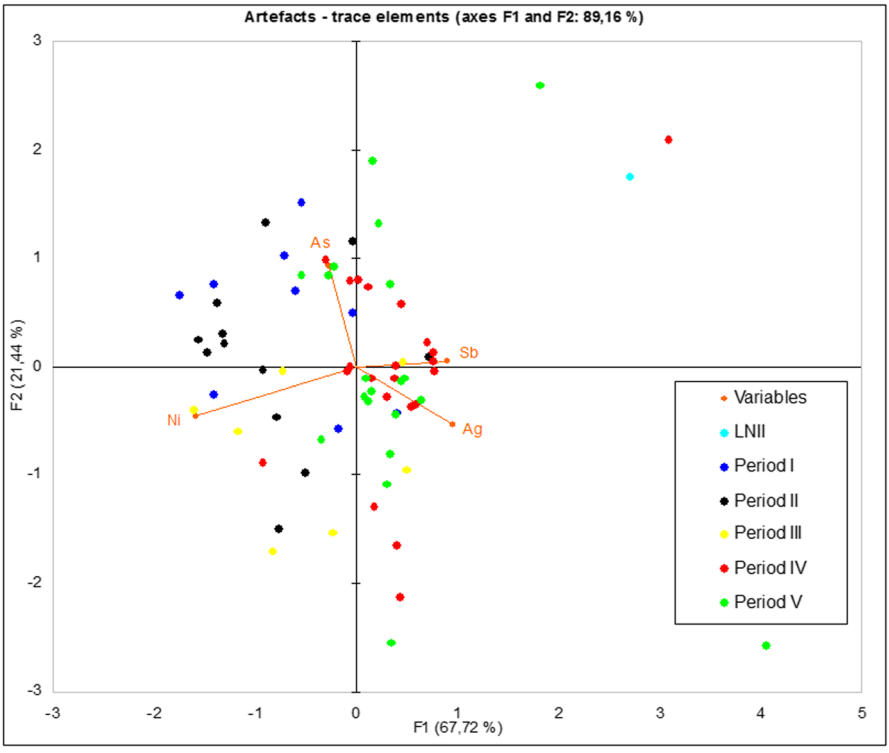

Fig. 11 Bronze Age finds from Sweden—PCA graph with wt% values of Ni, Ag, Sb, and As (centred log-ratio transformed)

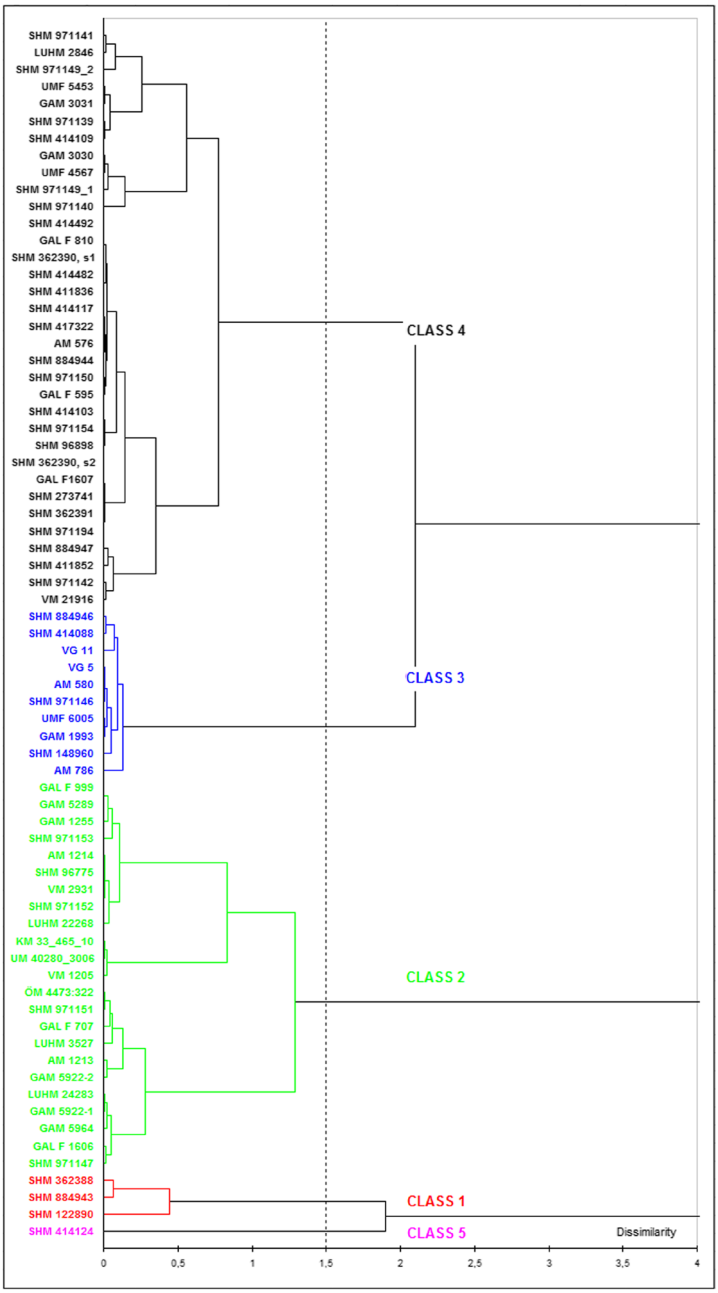

Fig. 12 Bronze Age finds from Sweden—AHC dendrogram on PC scores with wt% values of Ni, Ag, Sb, and As (centred log-ratio transformed). Level 1.5 truncation

Concerning the chemistry patterns, we have employed Variable Set 3. The PCA-AHC approach (Figs. 11 and 12) successfully demonstrates changes in these patterns through time. Five classes were isolated:

- Class 1 (3 observations): LNII—1, Period IV—1, Period V—1
- Class 2 (23 observations): Period I—6, Period II—10, Period III—5, Period IV—1, Period V—1
- Class 3 (10 observations): Period I—1, Period II—1, Period IV—4, Period V—4
- Class 4 (34 observations): Period I—2, Period II—1, Period III—2, Period IV—16, Period V—13
- Class 5 (1 observation): Period V—1

Although there is some overlap between the periods and the classes, Classes 1 and 5 group the finds from Periods IV–V almost exclusively, and Classes 3 and 4 are dominated by the observations from these periods. On the other hand, Class 2 mostly includes the finds from Periods I, II, and III. The Late Neolithic dagger goes together with the finds from Periods IV–V. The PCA graph in Fig. 11 (89.16% of the total variability) also implies that the contents of Sb and Ag are lower in the finds from Periods II–III (and the same seems to be true for Period I), while a majority of the later finds demonstrate higher amount of the trace elements in question. All this is in line with the remarks made by J. Ling and co-authors.

Case Study 3—the Nebra Hoard, Romanian, Hungarian, and Danish Bronze Age Artefacts

D. Berger and co-authors published results of new analyses of Early and Middle Bronze Age (c. 2000–1200 BC) bronze artefacts (34 observations) from Romania (Apa), Hungary (Hajdúsámson and Téglás), Germany (Nebra) and Denmark, together with previous research results for other Scandinavian Bronze Age finds. The main aim of their study was to discuss metal mixing patterns through the analysis of Pb, Cu, and Sn isotopes (Berger *et al.,* 2022a: 45–47, 48–48, Table 1, 50–51, Table 2, 9, 53–54, Table 3, 55). Pb isotope ratios and the chemistry of the studied finds were also compared with data for two copper ore deposits from Mitterberg in Austria and the Hron Valley in Slovakia (Berger *et al.,* 2022a: 55–56, Fig. 3, 57–59, 60, Fig. 5, 61). Based on these results, mixing and recycling scenarios were discussed (Berger *et al.,* 2022a: 57–58, Fig. 4, 61–62, 63–64, Figs. 6 and 7, 65–66, Figs. 8-9, 67–68). In our study, we examine relationships between the artefacts and the two deposits, comparing our results with observations made by D. Berger and colleagues (for previous research on these finds see also Pernicka *et al.,* 2020; Ling *et al.,* 2019: 3, Table 2; Pernicka *et al.,* 2016a: 34–35, Figs. 15-16, 36; Pernicka *et al.,* 2016b: 57–65). Deposit data was taken from relevant literature (Pernicka *et al.,* 2016a: 48–50, Table 3, 51–53, Table 4, 54, Table 5, 55, Tab, 6; Schreiner, 2007: 218–221, 227–230, 245–251).

Fig. 13 Pb isotopic ratios of the artefacts from Apa, Hajdúsámson, Téglás, Nebra, and Denmark against the background of copper deposits from Mitterberg and the Hron Valley (cf. Berger *et al.,* 2022a: 56, Fig. 3ab). Observation labels were added ▶

Concerning the Pb isotopic composition (Fig. 13), both deposits show both a reasonable separation and a strong overlapping zone. In the light of the remarks concerning relationships between ores and slags (Baron *et al.,* 2014: 670–672; Rademakers *et al.,* 2020: 11–17), it is also worth noting that in this case, Mitterberg slag observations plot in the same area as Mitterberg ore data. On the other hand, the slag data distribution is notably much less heterogeneous. Regarding possible artefact-deposit relationships, the Danish swords fall into two groups—the finds from Guldbjerg, Rind, and Valsømagle with less radiogenic values, and the sword from Stensgård with more radiogenic ones. The Téglás axe is close to the former group, while the chisel and the axe from Nebra, the Hajdúsámson sword, and another four axes are more related to the latter group. The remaining artefacts fall between these two groups. The Nebra, Hajdúsámson, and Téglás hoards are heterogeneous, while the Apa hoard (save one axe) seems more homogeneous. Some finds from Nebra, Stensgård, and Hajdúsámson can be isotopically classified to Mitterberg (one Apa axe may be related to a different Mitterberg lode). The swords from Guldbjerd, Rind, Valsømagle, and the Téglás axe can be related to the Hron Valley, while the remaining artefacts fall within the in-between zone. These finds may have been made from a mixture of metals from both ores (Berger *et al.,* 2022a: 56, Fig. 3ab, 57, 59; for observations on the Sn and Cu isotopic compositions see ibid., 57–58, 60–62, 63–68). Thus, the following scenario is likely:

- Mitterberg (11 observations): Hajdúsámson Axes 1, 3, 4, 7, 8, and the sword; Denmark Sword 5 (Stensgård) blade and hilt; Nebra chisel, axe and Sword 2 Rivet 2
- Hron (6 observations): Téglás axe; Denmark Swords 1–4 (Guldberg, Valsømagle, Rind); Nebra Sword 2 hilt
- in-between zone (16 observations): Apa Axes 1–3, and Swords 1–2; Hajdúsámson Axes 2, 5, 6, and 9; Téglás sword blade and hilt; Nebra Sky Disc, Sword 1 blade and rivet, and Sword 2 blade and Rivet 1

Regarding the chemistry of the artefacts and deposits (Fig. 14), the contents of impurities in the artefacts are basically low and on a similar level. Only the sword blade and the axe from Téglás demonstrate higher Ni contents and the highest concentrations of As and Sb. The Ag content in these artefacts is also high. All other finds display lower concentrations of As, Sb, and Ag. The Mitterberg deposits are low in Ag and Sb, while containing up to 1% Ni. The Hron Valley deposits are Ni-poor, but are richer in As, Ag, and Sb. A narrow overlapping zone exists between both deposits and most artefacts plot into it, while some match either Mitterberg or Hron. This match corresponds to the isotopic classification (Berger *et al.,* 2022a: 55–56, 59).

We first analyse Variable Set 1, focusing on the relationships between the artefacts and the deposits. There is both a reasonable separation between both deposits and an overlapping area, as can be seen in Fig. 15 (99.94% of the total variability). As in the case of the biplots with Pb isotopic ratios (Fig. 13), the

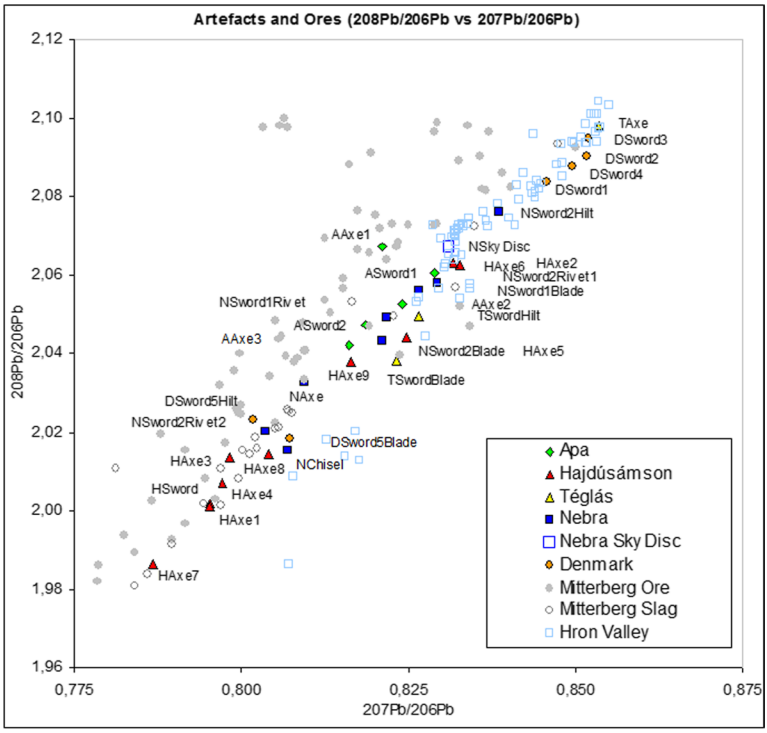
Artefacts and Ores (208Pb/206Pb vs 207Pb/206Pb)
208Pb/206Pb
207Pb/206Pb
2,12
2,10
2,08
2,06
2,04
2,02
2,00
1,98
1,96
0,775
0,800
0,825
0,850
0,875
TAxe
DSword3
DSword2
DSword4
DSword1
NSword2Hilt
AAxe1
NSky Disc
HAxe6
HAxe2
ASword1
NSword2Riv et1
NSword1Blade
NSword1Riv et
AAxe2
TSwordHilt
ASword2
AAxe3
NSword2Blade
HAxe5
HAxe9
TSwordBlade
NAxe
DSword5Hilt
NSword2Riv et2
DSword5Blade
HAxe3
HAxe8
NChisel
HSword
HAxe4
HAxe1
HAxe7
Apa
Hajdúsámson
Téglás
Nebra
Nebra Sky Disc
Denmark
Mitterberg Ore
Mitterberg Slag
Hron Valley

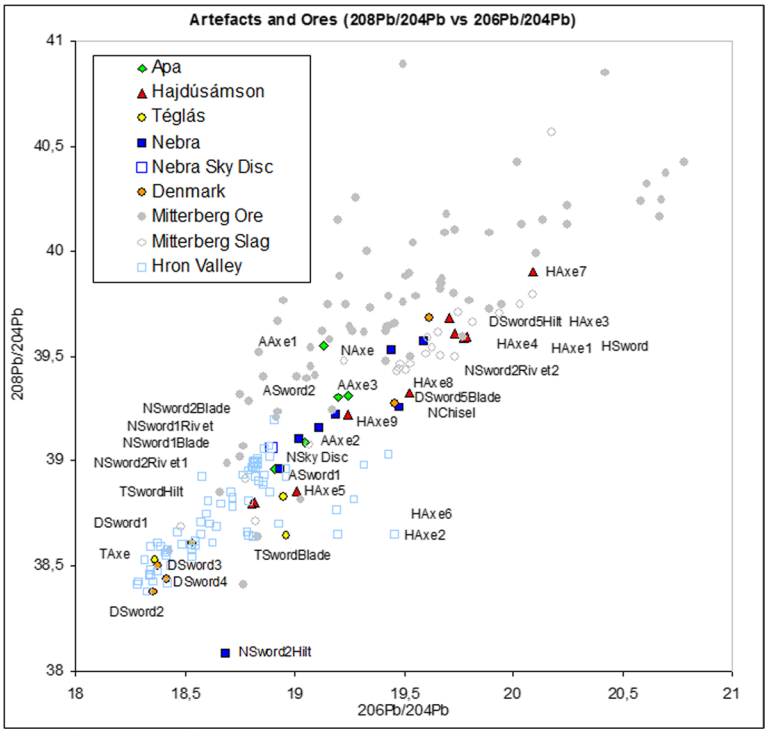
Artefacts and Ores (208Pb/204Pb vs 206Pb/204Pb)
208Pb/204Pb
206Pb/204Pb
41
40,5
40
39,5
39
38,5
38
18
18,5
19
19,5
20
20,5
21
Apa
Hajdúsámson
Téglás
Nebra
Nebra Sky Disc
Denmark
Mitterberg Ore
Mitterberg Slag
Hron Valley
HAxe7
DSword5Hilt
HAxe3
AAxe1
NAxe
HAxe4
HAxe1
HSword
NSword2Riv et2
ASword2
AAxe3
HAxe8
DSword5Blade
NSword2Blade
NChisel
NSword1Riv et
HAxe9
NSword1Blade
AAxe2
NSky Disc
NSword2Riv et1
ASword1
TSwordHilt
HAxe5
HAxe6
DSword1
HAxe2
TAxe
TSwordBlade
DSword3
DSword4
DSword2
NSword2Hilt

Fig. 14 Ratios of selected trace elements (normalised to 100% with Cu) in the artefacts from Apa, Hajdúsámson, Téglás, Nebra, and Denmark against the background of copper deposits from Mitterberg and the Hron Valley (cf. Berger *et al.,* 2022a: 60, Fig. 5). Observation labels were added ▶

greater homogeneity of Mitterberg slag data is also evident. As regards the artefacts, some plot clearly in the Hron Valley zone. These include the axe from Téglás; Swords 1–4 from Guldberg, Valsømagle, and Ring in Denmark; and Nebra Sword 2 hilt. Other artefacts imply a stronger affiliation to the Mitterberg zone (Hajdúsámson Axes 1, 3, 4, 7, 8, and the sword; Denmark Sword 5 (Stensgård) blade and hilt; Nebra chisel, axe, and Sword 2 Rivet 2), while the majority plot in the overlapping zone of both deposits.

The AHC isolates six classes which comprise the observations concerning the deposits in question as well as the artefact observations (Fig. 16). The composition of these classes (Table 2) confirms the results displayed in the PCA graph in Fig. 15 concerning possible artefact-deposit relationships, including the artefacts that were possibly made of mixed metal. It is also worth noting that the AHC was able to handle the aforementioned stronger homogeneity of the Mitterberg slag data, as these observations mostly (16 out of 22 cases) belong to Class 5.

Concerning the artefacts in question, this classification is almost in perfect agreement with what is implied by the Pb isotopic ratio biplots, Apa Axe 1 being the sole exception. D. Berger and co-authors propose that this observation may be related to another Mitterberg lode (Berger *et al.,* 2022a: 59). On the other hand, the Pb biplots could also imply its proximity to the overlapping zone, which is perhaps why it was classified so by the AHC. It is remarkable that less obvious artefact observations (Apa Axes 1 and 3, Apa Sword 2, Hajdúsámson Axe 9, Nebra Sword 2 hilt) are classified into the in-between group rather than into any deposit class. Classes 3, 4, and 6 are separate clusters that were isolated for distant deposit observations with no artefacts close to them.

For two reasons, it would be pointless to discuss possible relationships between the artefacts and the deposits using Variable Set 2. First, as shown in Figs. 13 and 14, the number of artefacts that can be related to one of the deposits based on the Pb isotopic ratios is much higher than that suggested by the trace element ratios, where most artefacts plot in the overlapping zone (Berger *et al.,* 2022a: 59). In other words, the discriminating power of Pb isotopic ratios is clearly superior in this case (Pernicka, 2014: 248–250; Artioli *et al.,* 2020: 2; however, chemistry can sometimes be more informative, Pernicka, 2014: 250; Pernicka *et al.,* 2016b: 67; Radivojević *et al.,* 2019: 139; see also, *e.g.* Albarède *et al.,* 2020: 2; Killick *et al.,* 2020: 91–92, 100–101). The other reason is the incompleteness of these deposit datasets. The entire Case Study 3 dataset includes 250 observations, out of which 34 are the artefacts and 216 are the deposits (137 Mitterberg and 79 Hron Valley). When working on the NA Pb isotope data, 35 observations were removed due to the absence of Pb isotope data (34 Mitterberg and 1 artefact). In a combined Pb isotope and chemistry dataset, 70 observations would be removed (1 artefact and 34 Mitterberg with no Pb isotope data; 22 Mitterberg and 13 Hron Valley with no chemistry data). It is obvious that the removal of observations

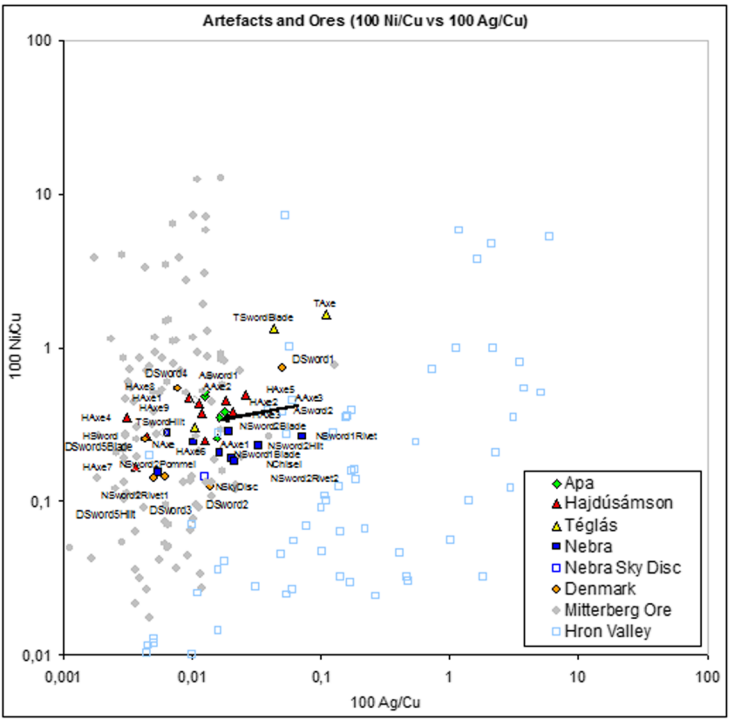
Artefacts and Ores (100 Ni/Cu vs 100 Ag/Cu)
100 Ni/Cu
100 Ag/Cu
100
10
1
0,1
0,01
0,001
0,01
0,1
1
10
100
TAxe
TSwordBlade
DSword1
DSword4
ASword1
AAxe2
HAxe5
AAxe3
HAxe2
ASword2
HAxe4
TSwordHilt
NSword2Blade
NSword1Rivet
HSword
DSword5Blade
NAxe
AAxe1
NSword2Hilt
HAxe6
NSword1Blade
HAxe7
NSword2Pommel
NChisel
NSword2Rivet2
NSkyDisc
NSword2Rivet1
DSword5Hilt
DSword3
DSword2
Apa
Hajdúsámson
Téglás
Nebra
Nebra Sky Disc
Denmark
Mitterberg Ore
Hron Valley

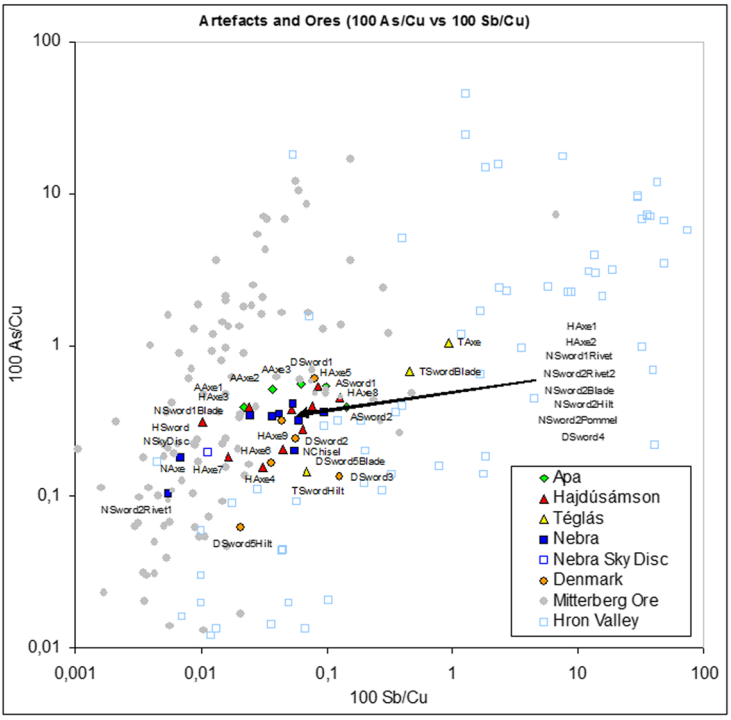
Artefacts and Ores (100 As/Cu vs 100 Sb/Cu)
100 As/Cu
100 Sb/Cu
100
10
1
0,1
0,01
0,001
0,01
0,1
1
10
100
TAxe
HAxe1
HAxe2
NSword1Rivet
NSword2Rivet2
NSword2Blade
NSword2Hilt
NSword2Pommel
DSword4
DSword1
AAxe3
AAxe2
HAxe5
TSwordBlade
AAxe1
ASword1
HAxe8
HAxe3
ASword2
NSword1Blade
HSword
NSkyDisc
HAxe9
DSword2
HAxe6
NChisel
DSword5Blade
NAxe
HAxe7
DSword3
HAxe4
TSwordHilt
NSword2Rivet1
DSword5Hilt
Apa
Hajdúsámson
Téglás
Nebra
Nebra Sky Disc
Denmark
Mitterberg Ore
Hron Valley

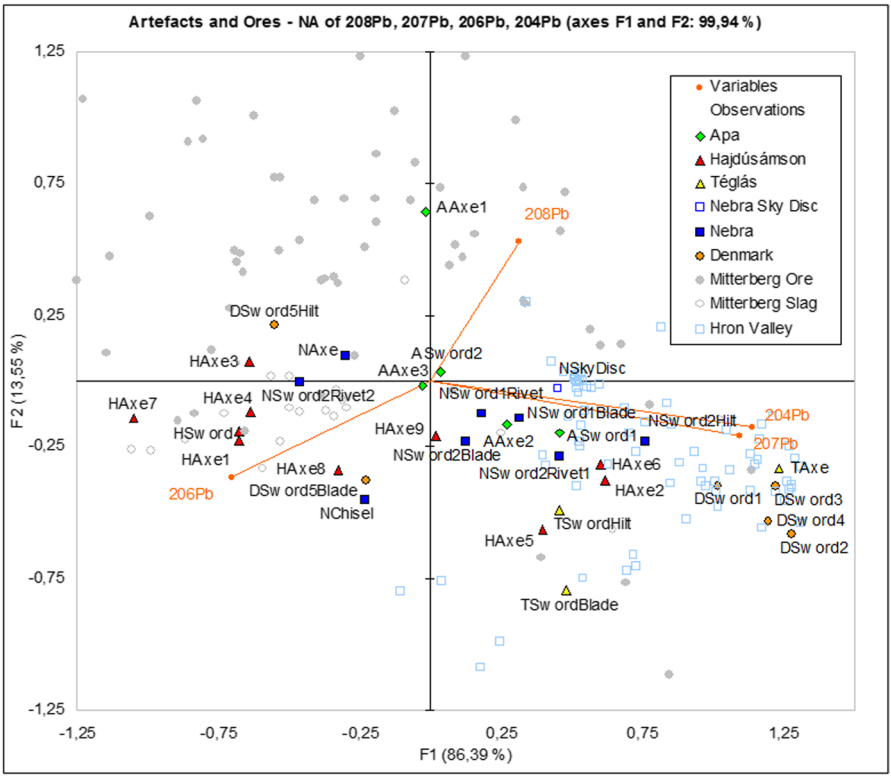

Fig. 15 Artefacts from Apa, Hajdúsámson, Téglás, Nebra, and Denmark against the background of copper deposits from Mitterberg and the Hron Valley—PCA graph with NA of ^{208}Pb, ^{207}Pb, ^{206}Pb, and ^{204}Pb (0–1 rescaled). Central part of the graph with artefact observations

from a multivariate dataset will inevitably affect relationships between the remaining ones and will eventually influence clustering results. Therefore, in this case, it is more sensible to solely compare both deposits using Variable Set 2.

The PCA graph (Fig. 17) implies a very good separation with a narrow overlapping zone. This impression seems even more trustworthy as the total variability on the PC1 and PC2 axes is high (90.90%). However, if PC3 (6.05%) is also considered (Fig. 18), a strong overlap becomes evident. This demonstrates how dangerous it is to assume a good separation between observations using a two-dimensional PCA graph alone, even if it contains over 90% of the information. For instance, C. Canovaro used 2D PCA graphs to discuss chemistry-based groups of ingots and other artefacts. However, the biplot axes contained only 52.0–66.6% of the variability (Canovaro, 2016: 35–36, 72–73, Fig. 5.2, 74, 78–79, Fig. 5.5, 90–91, Fig. 5.11). M. D. Glascock postulates "to include all PCs until the total percent of variance explained reaches an acceptable level. For a majority of archaeological work, this is about 90% of the variance" (Glascock, 2016: 14). However, as our example demonstrates, even 90% is not always enough. What is more, this case again stresses the

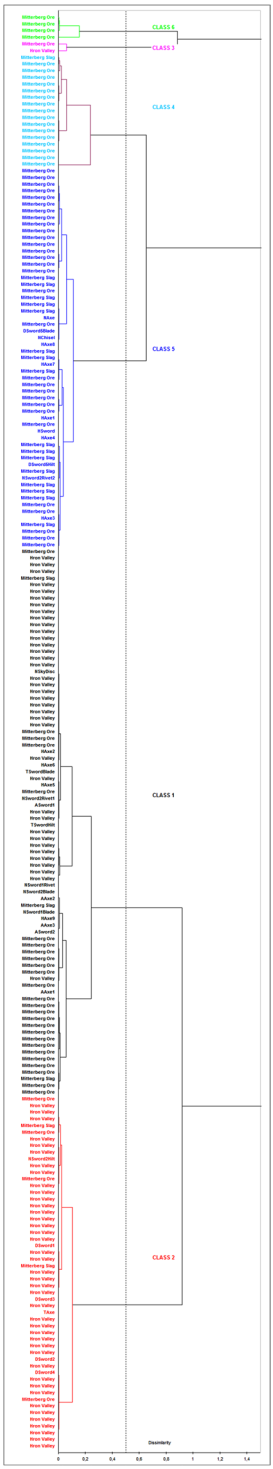

Fig. 16 Artefacts from Apa, Hajdúsámson, Téglás, Nebra, and Denmark against the background of copper deposits from Mitterberg and the Hron Valley—AHC dendrogram on PC scores with NA of ^{208}Pb, ^{207}Pb, ^{206}Pb, and ^{204}Pb (0–1 rescaled). Level 0.5 truncation

Table 2 PCA-AHC classification of the artefacts from Apa, Hajdúsámson, Téglás, Nebra, and Denmark and the copper deposits from Mitterberg and the Hron Valley

Class 1 81 observations (overlapping)	Class 2 53 observations (mainly Hron)	Class 3 2 observations (overlapping)	Class 4 18 observations (Mitterberg)	Class 5 57 observations (Mitterberg)	Class 6 4 observations (Mitterberg)
Hron Valley 37	Hron Valley 41	Hron Valley 1	Mitterberg Ore 17	Mitterberg Ore 30	Mitterberg Ore 4
Mitterberg Ore 25	Mitterberg Ore 4	Mitterberg Ore 1	Mitterberg Slag 1	Mitterberg Slag 16	
Mitterberg Slag 3	Mitterberg Slag 2			Hajdúsámson sword	
Apa Axe 1	Téglás axe			Hajdúsámson Axe 1	
Apa Axe 2	Nebra Sword 2 hilt			Hajdúsámson Axe 3	
Apa Axe 3	Denmark Sword 1 (Guldbjerg)			Hajdúsámson Axe 4	
Apa Sword 1	Denmark Sword 2 (Valsømagle)			Hajdúsámson Axe 7	
Apa Sword 2	Denmark Sword 3 (Valsømagle)			Hajdúsámson Axe 8	
Hajdúsámson Axe 2	Denmark Sword 4 (Rind)			Nebra chisel	
Hajdúsámson Axe 5				Nebra axe	
Hajdúsámson Axe 6				Nebra Sword 2 Rivet 2	
Hajdúsámson Axe 9				Denmark Sword 5 (Stensgård) blade	
Téglás sword hilt				Denmark Sword 5 (Stensgård) hilt	
Téglás sword blade					
Nebra Sky Disc					
Nebra Sword 2 blade					
Nebra Sword 1 blade					
Nebra Sword 2 Rivet 1					
Nebra Sword 1 rivet					

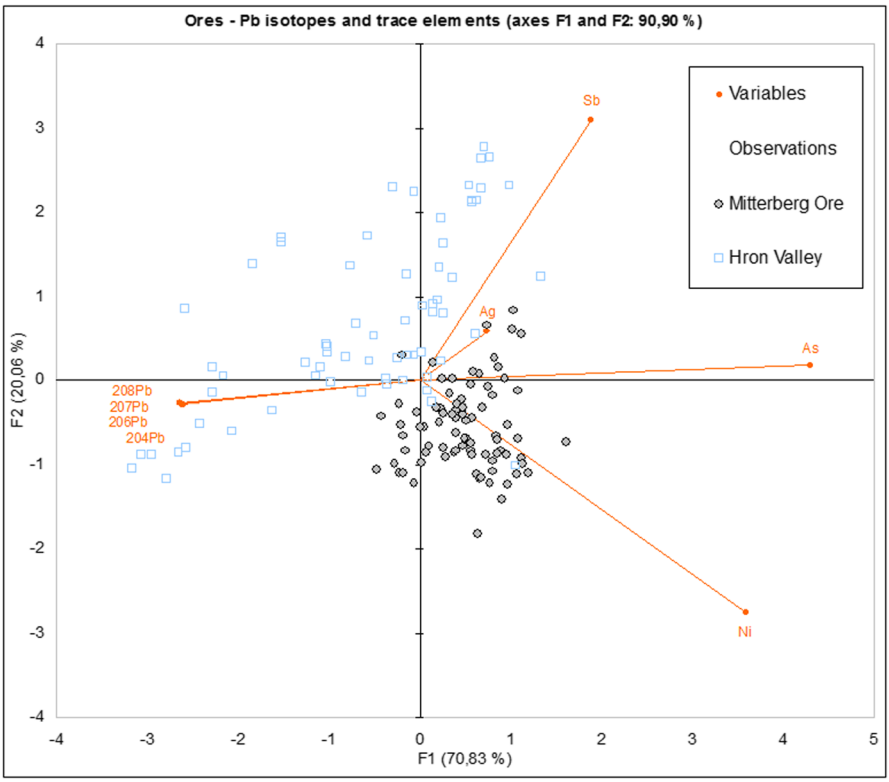

Fig. 17 Copper ore deposits from Mitterberg and the Hron Valley—PCA graph with wt% values of ^{208}Pb, ^{207}Pb, ^{206}Pb, ^{204}Pb, Ni, As, Ag, and Sb (centred log-ratio transformed)

AHC reliability as a cluster identification method and confirms a need to use it to display true relationships between analysed observations.

The AHC isolates five classes (Fig. 19). Three of these are exclusively the Hron Valley (Class 1—12 observations, Class 2—13, Class 4—16). Class 3 is a major part of the overlapping zone (Hron Valley—22, Mitterberg—48), while Class 5 is almost exclusively Mitterberg (33), with only three Hron Valley observations. A comment must also be made on the result that was produced by the automatic truncation of the dendrogram. The result brought together Classes 1 and 2 (both Hron Valley), with no change in Classes 3, 4, and 5. In this case, however, it is more sensible to split the Hron Valley observations into three classes, as suggested by the PCA graphs. All in all, the results produced by PCA-AHC on Variable Set 2 are fully consistent with what is implied by the Pb isotopic ratio and chemistry biplots (Figs. 13 and 14).

Case Studies 4 and 5—Finding a Way Out of the Data Maze

In Case Study 4, we have examined how the PCA-AHC handles a large dataset with more than 4500 Pb isotopic signatures of ore deposits. This corresponds

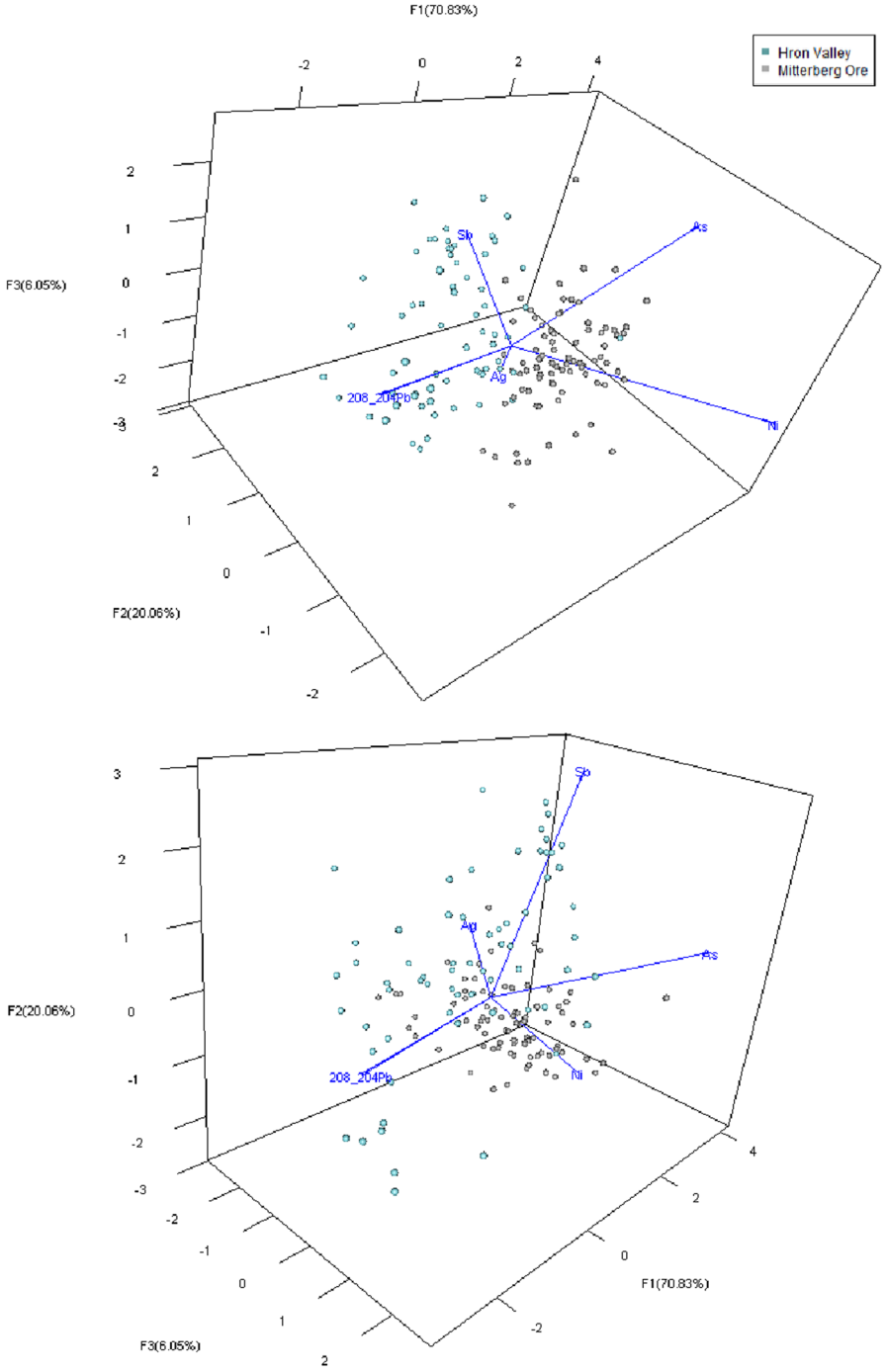

Fig. 18 Copper ore deposits from Mitterberg and the Hron Valley—3D PCA graphs with wt% values of ^{208}Pb, ^{207}Pb, ^{206}Pb, ^{204}Pb, Ni, As, Ag, and Sb (centred log-ratio transformed)

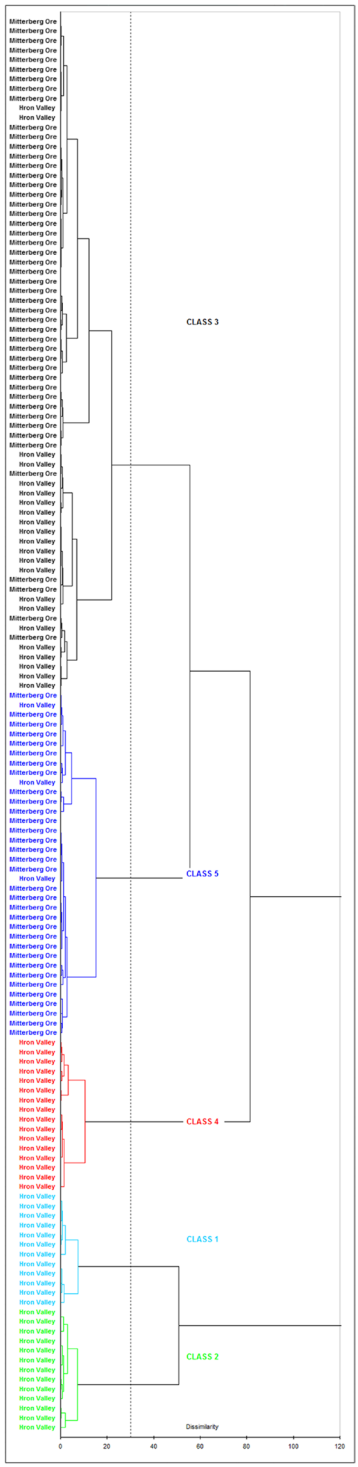

Fig. 19 Copper ore deposits from Mitterberg and the Hron Valley—AHC dendrogram on PC scores with wt% values of ^{208}Pb, ^{207}Pb, ^{206}Pb, ^{204}Pb, Ni, As, Ag, and Sb (centred log-ratio transformed). Level 30 truncation

to a real-life scenario, in which we want to suggest artefact provenance patterns against the background of all possible candidate deposits. We have used the database provided by D. J. Killick and colleagues (Killick *et al.,* 2020: Electronic Data S1) and have selected the "Europe&Mediterranean" dataset. This database is of course not ideal, as its main aim is to inform archaeologists in which parts of the world Pb isotopic analyses can produce the best results (Killick *et al.,* 2020: 87). It is not complete and it contains Pb isotopic data on minerals that could be used for smelting of other metals than copper, as well as data on general minerals. Moreover, it comprises observations on ore deposits mined in Prehistory or the Middle Ages, but also data obtained by present-day geological drillings. Apart from that, although it provides data on minerals that were analysed, in most cases the geological context information is missing (Prof. David J. Killick, personal communication). It would therefore require completion and pre-filtering when used for provenance studies of actual archaeological finds. Thus, we simply use this database as a large pool of strongly overlapping data and examine whether the method is able to correctly group observations. We have randomly selected a copper ore deposit from Sierra El Aramo in Spain, which is numerically strong enough, as it includes 20 observations (see Electronic Supplement, Case Study 4, Sheet "Europe&Mediterranean STEP 1", Obs. Nos. 981–1000). Then, we have conceptualised two theoretical artefacts of unspecified chronology. An obvious advantage of such artefacts is that we can be absolutely certain that they derive from their parent ore deposit. The Pb isotopic composition of Artefact 1 is an average of 12 observations from the main body of this deposit. An artefact being an average of all observations could also be imagined, but as the Pb isotopic data of this deposit has some outliers, we have assumed that such a scenario would not be very realistic. Artefact 2 replicates the Pb isotopic composition of Obs. 986 from the El Aramo deposit (see Electronic Supplement, Case Study 4, Sheet "El Aramo for PCA" and Sheet "Europe&Mediterranean STEP 1", Artefact 1—Obs. 4525; Artefact 2—Obs. 4526). Then, we have examined whether the proposed method correctly assigns our artefacts to their parent ore deposit. As we use the "unsupervised" approach (see the remarks in Section "Advantages of the Statistical Treatment, its Possible Limitations and Importance of Input Data"), Artefact 2 should certainly end up in a class with at least one El Aramo deposit observation (that is, its parent Obs. 986), so its presence in the dataset is only intended to test the performance of the method when applied to a large dataset.

In Case Study 4, we use Variable Set 1, that is, NA values of all Pb isotopes after 0–1 rescaling. The multi-step PCA-AHC analysis includes the following procedures:

(1) 0–1 rescaled values of all observations are processed by PCA and obtained PC scores are processed by AHC in order to isolate classes
(2) class or classes containing our artefact observations are selected for further examinations, thus forming a new dataset or datasets
(3) after a class is selected, the NA values of individual observations in this new dataset are 0–1 rescaled again. This is not absolutely necessary but allows for a better examination of dissimilarities between observations. If 0–1 rescaling is omitted, these dissimilarities become so small in the subsequent steps that they

can pose computational problems, although eventual results proved to be the same

(4) a new PCA and then AHC is conducted and a new smaller class or classes containing our artefact observations are selected

(5) the class selection and PCA-AHC analyses are repeated for each new class(es) until a "clean" class is obtained, that is, a class that solely contains observations on the artefact(s) in question and observations on only one possible parent deposit.

In this case, it is of course possible that two final classes are obtained, each for one artefact. This would occur if Artefact 1 (being an average of several observations from its parent deposit) eventually proved more similar to other deposit observations than to its parent El Aramo ones. What is more, it can never be excluded that an initial dataset will contain more than one observation with identical Pb isotopic compositions but coming from different deposits. In such a scenario, neither of our artefacts could be provenanced unequivocally, as Artefact 2 would end up in a class with its parent El Aramo observation and identical observations from other deposits. Eventually, due to the well-known strong overlap of Pb isotopic data and considerable heterogeneity even within one ore body, the number of deposit observations in the final class or classes will inevitably be much lower than that in the entire parent deposit.

In the discussed case, the analysis encompassed six steps. Details can be found in the Supplementary Materials (see Electronic Supplement, Case Study 4, Sheets "Europe&Mediterranean STEP 1" to "Europe&Mediterranean STEP 6"), and here, we only briefly report on the obtained results. Out of more than 4500 initial observations, Step 1 selected a large Class 1 (4237 observations). However, after Step 2, the number of observations strongly decreased to 102 (Class 5), including 14 El Aramo deposit observations (out of the initial 20) and both Artefacts 1 and 2. It is worth noting that this class contained copper-bearing minerals in a vast majority of cases. After Step 3, a new Class 1 (49 observations in total) was obtained with 12 El Aramo deposit observations and both artefacts. This class was processed in Step 4. What is more, although 10 observations other than El Aramo concerned Spanish deposits, too, this class also included ore bodies from Italy, France, England, and other countries. This obviously confirms the fact that even deposits that are very distant in terms of geography can be very similar (see Electronic Supplement, Case Study 4, Sheet "Europe&Mediterranean STEP 4"). After Step 4, both Artefacts 1 and 2 were still in the same class (Class 3—15 observations altogether, including eight from the El Aramo deposit). After Step 5, only five observations (two from the El Aramo deposit, Artefacts 1 and 2, as well as an observation from Cerro Minado in Spain) forming Class 4 were selected. The final Step 6 separated this class into a new Class 1 with two El Aramo deposit observations and both artefacts and Class 2 with the aforementioned one Cerro Minado deposit observation. Apart from the aforementioned remarks concerning the deposit heterogeneity, the fact that only two El Aramo deposit observations are present in the final class is of no surprise for yet another reason. Namely, when traditional biplots are used, a provenance hypothesis is proposed on the

basis of proximities of artefact observations to individual deposit observations, rather than to "averages" of the entire deposit.

Case Study 5 has two main objectives. The first one is to study a real archaeological artefact, while the other is to demonstrate the method's performance on another non-ferrous metal, that is, lead. For this purpose, an Augustan-Tiberian Period lead ingot (D-137/21) from a Roman legionary camp in Haltern (North Rhine-Westphalia, Germany) was selected. This 64 kg heavy artefact is particularly well-suited for such a study. It has a narrow chronology (12 BC–9 AD), and both its find place and a "L(egio) XIX" mark clearly indicate its Roman provenance. M. Bode and colleagues argue that in most cases such ingots were cast at mining sites. Furthermore, these researchers say that lead scrap recycling after the retreat of Roman legions from this part of Germania is not very likely (Bode *et al.,* 2009: 178, 180, Table 1, 190). The provenance of the lead in this ingot was investigated by M. Bode and co-authors against the background of deposits from lead-mining districts in Germania (the Bensberg district in Bergisches Land, the Brilon district in Sauerland, as well as the Mechernicher Bleiberg and the Aachen-Stolberg districts in the Northwestern Eifel region) and in the Iberian Peninsula. It was eventually proposed that the metal came from Roman mines in the Bensberg district in Bergisches Land in North Rhine-Westphalia. These mines were still under the Roman control after the disastrous defeat in 9 AD (Bode *et al.,* 2009: 182–184, 187, Table 3, 188–190, 191, Fig. 6).

This ingot has recently been studied by S. De Ceuster and P. Degryse using the KDE-based approach. These researchers included a much larger database of ore deposits, with ore bodies from Greece, Egypt, Thrace, Macedonia, England, Scotland, Wales, Italy, Spain, and Turkey. In contrast, none of the German mining districts that were used by M. Bode and co-authors was considered. Instead, the only assemblage of German ore bodies included by S. De Ceuster and P. Degryse was that from the Siegerland region in North Rhine-Westphalia. As a result, they suggested that the "L(egio) XIX" ingot from Haltern was made of metal from Siegerland (De Ceuster & Degryse, 2020: 113, Fig. 3).

The selection of this region can be debated. One possible reason may have consisted in the fact that the KDE method works better with larger data bodies, which is why these researchers included only ore deposits with data available for at least 20 ore samples (De Ceuster & Degryse, 2020: 109, 111). In fact, the number of observations for the ore bodies used by M. Bode and colleagues is less than 20 in most cases, and for the Bensberg district, there are only three observations (Bode *et al.,* 2009: 185–186, Table 2). In contrast, the Siegerland dataset includes nearly 40 observations (Durali-Mueller *et al.,* 2007: 1558–1559, Table 1, also with data from other neighbouring regions). In our study, we have decided not to use the Siegerland data, chiefly because of the lack of archaeological evidence of Roman Period lead mining in this region (Dr Michael Bode and Dr Manuel Zeiler, personal communication; Zeiler *et al.,* 2016, 2018). Instead, we have included the German ore deposits that were used by M. Bode and colleagues. Regarding the other deposits that were considered by S. De Ceuster and P. Degryse, most of them can be found in an open-access GlobaLID database (Dra Sarah De Ceuster, personal communication; the database is available at https://globalid.dmt-lb.de/,

see Klein *et al.,* 2022; Westner *et al.,* 2021) and in the aforementioned dataset published by D. Killick and colleagues (Killick *et al.,* 2020: Electronic Data S1). Missing deposits were added from available literature (Wagner *et al.,* 1985, 1986; Scaife *et al.,* 2008; Seeliger *et al.,* 1985). The resulting database was pre-filtered, and only lead-bearing minerals (mainly galena) were retained. The final dataset contained more than 2000 observations.

The procedure was identical as in Case Study 4, so it is not restated here. Details are available in the Supplementary Materials (see Electronic Supplement, Case Study 5, Sheets "DATABASE STEP 1" to "DATABASE STEP 4"). In Step 1, Class 1 with 873 observations was isolated, including the "L(egio) XIX" ingot, while after Step 2 only 110 observations were retained (Class 1). After Step 3, this number was reduced to 19 (Class 3). In addition to the studied ingot, this class included two observations from the Bensberg district in Bergisches Land, but also those for galena deposits in Sardinia, Scotland, and Wales. The final Step 4 divided this class into nine new ones. The lead ingot went into Class 1, together with the aforementioned two observations from the Bensberg district and no other ore deposit observations. On these grounds, we can conclude that the PCA-AHC approach has successfully confirmed the ingot provenance as proposed by M. Bode and colleagues. Although this study was arguably easier than the previous case due to the much smaller dataset, a possible pitfall was posed by the fact that the number of observations in the Bensberg deposit was merely three. Therefore, they could have easily got lost in the data maze, which means that the "L(egio) XIX" ingot would have been classified to another very similar ore body. This can be considered a strength of the proposed approach compared with the KDE method. PCA-AHC is in no way limited by the number of observations for a given ore deposit, as it does not use the information on the deposit group (see Section "Advantages of the Statistical Treatment, its Possible Limitations and Importance of Input Data"). In the method proposed by S. De Ceuster and P. Degryse, KDE was used in a "supervised" manner, that is, provenance probabilities were calculated for groups of data (deposits). These groups were quite large in most cases, encompassing entire regions or countries (De Ceuster & Degryse, 2020: 112, Fig. 2, 113, Fig. 3, 114, Fig. 4). Bearing in mind the limitations mentioned by these researchers regarding the minimum number of observations, it could be asked how KDE would handle a deposit with as little Pb isotopic data available as in the Bensberg district deposit.

Case Studies 4 and 5 clearly demonstrate the ability of the PCA-AHC approach to disentangle individual observations from a true maze of a few thousand strong and considerably overlapping datasets and to correctly assign them to their parent ores. What is more, it can be well seen in the subsequent analytical steps how the PCA-AHC "deconstructed" the El Aramo deposit and retained only those observations that were the closest to the artefacts under study. It is also worth noting that the entire operation took less than one working day for each case study. More time would obviously be needed to discuss more artefacts, especially in case each of these would eventually be matched with a different ore deposit. In our opinion, however, the required workload would still be lower than that needed for producing and comparing multiple biplots with various combinations of Pb isotopic ratios (*e.g.* Ling *et al.,* 2014: 119 mentions about 85 plots). Moreover, the latter

would be much more prone to human bias and error than a method which is based on mathematical calculations.

Conclusions

Based on the aforementioned case studies, we have demonstrated that the PCA-AHC approach is also viable in provenance studies of non-ferrous archaeological metal with the use of Pb isotopic ratios and chemistry data. In line with what was said by M. Radivojević and her colleagues (Radivojević *et al.,* 2019: 136), PCA-AHC can be a valuable addition to the traditional biplot-based approach. This method can facilitate research and save time and trouble related to comparing multiple graphs. The process of data conversion (from ratios to NAs and then to weight concentrations) and transformation took merely a couple of hours for each case study. These transformations can also be largely automated in Excel or R. Even if counted together with the time needed for PCA-AHC calculations, the analysis proceeded faster when compared with the generation of multiple biplots and subsequent cross-comparisons between them. Thus, this method (with Variable Set 1) can be applied in the initial deposit selection process, or, as in Case Studies 4 and 5, it can be used standalone in many pre-filtering steps until final provenance hypotheses are proposed (as, *e.g.* in Dillmann *et al.,* 2017). Case Studies 4 and 5 clearly demonstrate that neither the numerical strength of the dataset nor a considerable data overlap is an obstacle here, and both these factors are obviously crucial in a real-life scenario. As remarked above, a combination of Pb isotopic and chemistry data can sometimes provide better results in provenance studies, and our method allows for an effective combination of both types of data without a need for a separate study of Pb isotopic ratios and chemistry graphs. Analogous to the KDE-based approach proposed by S. De Ceuster and P. Degryse, our method also offers a way for both mathematical and visual identification of provenance patterns and mixing scenarios. Such an approach can more reliably remove possible human error, which is likely to occur in cases of visual identifications solely based on multiple graphs. Another crucial advantage of our method is that readers can easily check and verify the proposed results, as we provide all data used in our study (both concerning the analysed artefacts and deposit bodies as possible sources). The latter is regrettably not a standard practice in Pb isotopic studies of archaeological artefacts. It is not always possible to check and verify results in many biplot-based studies, where it would be necessary to supply all the analysed graphs in order to fully convince the audience that the obtained result is trustworthy. Yet another strength is the fact that this method is open for any new variables which can be brought to weight units. A new dataset can be prepared, and the results it produces can be compared with those obtained with previous datasets. Moreover, in Case Study 3, we have demonstrated why interpretations which are solely based on PCA graphs can be misleading, and the AHC is thus an indispensable completion. The AHC classification can also help clarify less obvious cases, albeit certainly not all of these, such as too strongly overlapping data or

mixing of metal from multiple sources. Regarding metal mixing, in Case Study 3, our method has proven to be able to identify the artefacts that were possibly made of metal from two sources. In Case Study 4, if an artefact made of metal from two different sources were analysed, it could be supposed that it would eventually go into a class containing observations belonging to these deposits. An obvious prerequisite is that both sources are present in the initial dataset. On the other hand, if an artefact ends up in a solitaire class on its own, this may imply that its parent deposit is not present among the analysed data. Naturally, both hypotheses need to be tested and verified.

A practical application of the proposed method is not without problems. As rightfully remarked by D. J. Killick and colleagues, advanced statistical methods are useful, but they will not replace traditional geochemical approaches in archaeological provenance studies with the use of Pb isotopic ratios. Therefore, it will always be necessary to examine the geological history of ore formation in the regions to be analysed (Killick *et al.,* 2020: 87; Baron *et al.,* 2014: 669). It can be anyway seen that more recent databases such as GlobaLID contain much more geological data (tectonic unit, deposit type, or geological period and age) than earlier ones (*e.g.* OXALID), where only mineral types are mentioned. No method, no matter how statistically advanced, will be able to show a sensible pattern if data overlap is too strong. Therefore, a regional variation of Pb isotopic ratios must always be taken into consideration (Killick *et al.,* 2020: 94). Another major impediment is a still insufficient number of ore deposits with complete Pb isotopic and chemistry data. Indeed, a provenance study should ideally consider the nearby mines that were being exploited at the time of the artefact's creation. However, many regions only have a weak coverage for copper (let us quote for example the case of France for which the majority of the studied deposits concern lead–zinc and not copper). A postulate of standardisation, rationalisation, and making existing datasets publicly available has recently been discussed by G. Artioli and co-authors (Artioli *et al.,* 2020: 23) and various open-access databases are currently under development, such as the aforementioned GlobaLID (see also a recently published database by C. Tomczyk, Tomczyk, 2022).

What is more, if used uncritically in a belief that it is a skeleton key capable of opening every door, this approach can easily turn into a razor in a monkey's hand and produce confusing results. This can occur, *e.g.* if researchers analyse datasets with too many incomplete observations jointly. In such a situation, it is recommended to use separate Pb isotopic and chemistry datasets and then to compare results. The same applies to cases where the Pb isotopic composition discriminates well between individual ore deposits and/or artefacts, while their chemistry overlaps (and vice versa). What is more, the proposed method can perhaps be of use in provenance studies of other non-ferrous metals, such as silver. Of course, some obvious reservations must be borne in mind, such as the fact that the Pb content in silver can be related not only to argentiferous lead ores used for silver smelting, but also to lead addition as part of metal purification in the cupellation process (Pernicka, 2014: 259). It also seems reasonable to call for a search of other multivariate approaches that could be potentially valuable tools in provenance studies on archaeological non-ferrous metal. Eventually, it should become

a standard that each study is provided with a full dataset, both concerning artefacts under discussion and possible metal sources.

Supplementary Information The online version contains supplementary material available at https://doi.org/10.1007/s10816-022-09598-y.

Acknowledgements Thanks must go to many persons for their help and support. Prof. Michael Brauns kindly provided an important suggestion for the procedure of dataset building. Prof. David J. Killick supplied additional valuable information concerning his dataset, while Prof. Zofia Stos-Gale and Prof. Gilberto Artioli shared their opinions on the combination of Pb isotopic and chemistry data. Dr Ewelina Mińta-Jakubowska provided an unpublished dataset on which the proposed approach was initially tested. Prof. Ernst Pernicka kindly provided the Mitterberg deposit data, while Dr Daniel Berger generously supplied the difficult-to-access publication with the Hron Valley deposit data. Dr Michael Bode and Dr Manuel Zeiler commented on the chronology of German lead-bearing deposits, and Dra Sarah De Ceuster provided information on the dataset used in her study. Dr Annelise Binois and Ms Corinne Watts proofread the final version of the text. Eventually, we are greatly indebted to four anonymous reviewers whose insightful and supportive comments significantly improved this paper.

Author Contribution Céline Tomczyk and Grzegorz Żabiński conceptualised the proposed research method. Grzegorz Żabiński carried out the calculations and prepared a draft of the paper. Céline Tomczyk revised the draft and added numerous important remarks concerning geological and technological aspects of provenance studies using Pb isotopes and chemistry data. Both authors read and approved the final manuscript.

Data Availability All data generated or analysed during this study are included in this published article [and its supplementary information files].

Declarations

Conflict of Interest The authors declare no competing interests.

References

Albarède, F., Blichert-Toft, J., Gentelli, L., Milot, J., Vaxevanopoulos, M., Klein, S., Westner, K., Birch, T., Davis, G., & de Callataÿ, F. (2020). A miner's perspective on Pb isotope provenances in the Western and Central Mediterranean. *Journal of Archaeological Science, 121*, 105194. https://doi.org/10.1016/j.jas.2020.105194

Albarède, F., Desaulty, A.-M., & Blichert-Toft, J. (2012). A geological perspective on the use of Pb isotopes in archaeometry. *Archaeometry, 54*(5), 853–867. https://doi.org/10.1111/j.1475-4754.2011.00653.x

Aragón, E., Montero-Ruiz, I., Polzer, M. E., & van Duivenvoorde, W. (2022). Shipping metal: Characterisation and provenance study of the copper ingots from the Rochelongue underwater site (seventh–sixth century BC), West Languedoc France. *Journal of Archaeological Science: Reports, 41*, 103286. https://doi.org/10.1016/j.jasrep.2021.103286

Artioli, G., Canovaro, C., Nimis, P., & Angelini, I. (2020). LIA of prehistoric metals in the Central Mediterranean area: A review. *Archaeometry, 62*(S1), 53–85. https://doi.org/10.1111/arcm.12542

Artioli, G., Angelini, I., Kaufmann, G., Canovaro, C., Dal Sasso, G., & Villa, I. M. (2017). Long distance connections in the Copper Age: New evidence from the Alpine Iceman's copper axe. *PLoS ONE, 12*(7), e0179263. https://doi.org/10.1371/journal.pone.0179263

Athanassov, B., Chernakov, D., Dimitrov, K., Krauss, R., Popov, H., Schwab, R., Slavchev, V., & Pernicka, E. (2020). A new look at the Late Bronze Age oxhide ingots from the Eastern Balkans. In J. Maran, R. Bajenaru, S.-C. Ailincai, A.-D. Popescu & S. Hansen (Eds.), *Objects, Ideas and Travellers. Contacts between the Balkans, the Aegean and Western Anatolia during the Bronze and Early Iron Age* (pp. 299–356). Verlag Dr. Rudolf Habelt GMBH. https://www.researchgate.net/publication/342437997 Accessed 15 Aug 2022

Baron, S., Tamas, C. G., & Le Carlier, C. (2014). How mineralogy and geochemistry can improve the significance of Pb isotopes in metal provenance studies. *Archaeometry, 56*(4), 665–680. https://doi.org/10.1111/arcm.12037

Baxter, M. (2015). Notes on quantitative archaeology and R. https://www.researchgate.net/publication/277931925 Accessed 20 Nov 2018

Baxter, M. J. (1999). On the multivariate normality of data arising from lead isotope fields. *Journal of Archaeological Science, 26*, 117–124. https://www.academia.edu/16302169. Accessed 25 Apr 2022

Baxter, M. & Hancock, R. G. V. (2018). Provenancing metal artefacts and multivariate statistics. https://www.academia.edu/8417998. Accessed 7 Mar 2020

Baxter, M. J., Beardah, C. C., & Wright, R. V. S. (1997). Some archaeological applications of Kernel Density Estimates. *Journal of Archaeological Science, 24*, 347–354. https://doi.org/10.1006/jasc.1996.0119

Begemann, F., Schmitt-Strecker, S., Pernicka, E., & Lo Schiavo, F. (2001). Chemical composition and lead isotopy of copper and bronze from Nuragic Sardinia. *European Journal of Archaeology, 4*(1), 43–85. https://doi.org/10.1179/eja.2001.4.1.43

Bérard, E., Dillmann, P., Disser, A., Vega, E., Verna, C., & Toureille, V. (2022a). The medieval bombards of Meaux: Manufacturing processes and supply of the metal. *Journal of Archaeological Science: Reports, 41*, 103307. https://doi.org/10.1016/j.jasrep.2021.103307

Bérard, E., Dillmann, P., Renaudeau, O., Verna, C., & Toureille, V. (2022b). Fabrication of a suit of armour at the end of Middle Ages: An extensive archaeometallurgical characterization of the armour of Laval. *Journal of Cultural Heritage, 53*, 88–99. https://doi.org/10.1016/j.culher.2021.11.008

Bérard, E., Pécheyran, Ch., Dillmann, P., Leroy, S., Vega, E., Williams, A., Verna, C., & Toureille, V. (2020). Ancient armour provenance by LA-ICP-MS analysis of microscopic slag inclusions. *Journal of Analytical Atomic Spectrometry, 35*, 2582–2593. https://doi.org/10.1039/D0JA00259C

Berger, D., Brügmann, G., Bunnefeld, J.-H., & Pernicka, E. (2022a). Identifying mixtures of metals by multi-isotope analysis: Disentangling the relationships of the Early Bronze Age swords of the Apa-Hajdúsámson type and associated objects. *Archaeometry, 64*(S1), 44–74. https://doi.org/10.1111/arcm.12714

Berger, D., Wang, Q., Brügmann, G., Lockhoff, N., Roberts, B. W., & Pernicka, E. (2022b). The Salcombe metal cargoes: New light on the provenance and circulation of tin and copper in Later Bronze Age Europe provided by trace elements and isotopes. *Journal of Archaeological Science, 138*, 105543. https://doi.org/10.1016/j.jas.2022.105543

Birch, T. & Martinón-Torres, M. (2014). The iron bars from the 'Gresham Ship': Employing multivariate statistics to further slag inclusion analysis of ferrous objects. *Historical Metallurgy Society, 48*, 69–78. https://www.hmsjournal.org/index.php/home/article/download/92/90 Accessed 2 Jun 2019

Birch, T., Westner, K. J., Kemmers, F., Klein, S., Hofer, H. E., & Seitz, H.-M. (2020). Retracing Magna Graecia's silver: Coupling lead isotopes with a multi-standard trace element procedure. *Archaeometry, 62*(1), 81–108. https://doi.org/10.1111/arcm.12499

Bode, M., Hauptmann, A., & Mezger, K. (2009). Tracing Roman lead sources using lead isotope analyses in conjunction with archaeological and epigraphic evidence – a case study from Augustan/Tiberian Germania. *Archaeological and Anthropological Sciences, 1*, 177–194. https://doi.org/10.1007/s12520-009-0017-0

Brauns, M., Yahalom-Mack, N., Stepanov, I., Sauder, L., Keen, J., & Eliyahu-Behar, A. (2020). Osmium isotope analysis as an innovative tool for provenancing ancient iron: A systematic approach. *PLoS ONE, 15*(3), e0229623. https://doi.org/10.1371/journal.pone.0229623

Brauns, M., Schwab, R., Gassmann, G., Wieland, G., & Pernicka, E. (2013). Provenance of Iron Age iron in southern Germany: A new approach. *Journal of Archaeological Science, 40*, 841–849. https://doi.org/10.1016/j.jas.2012.08.044

Bray, P. (2022). Is a focus on 'recycling' useful? A wider look at metal mutability and the chemical character of copper alloys. *Archaeometry, 64*(S1), 87–97. https://doi.org/10.1111/arcm.12753

Bray, P., Cuénod, A., Gosden, C., Hommel, P., Liu, R., & Pollard, A. M. (2015). Form and flow: The 'karmic cycle' of copper. *Journal of Archaeological Science, 56*, 202–209. https://doi.org/10.1016/j.jas.2014.12.013

Brügmann, G., Berger, D., Nessel, B., & Pernicka, E. (2018). Chemische Zusammensetzung und Zinn- und Bleiisotopenverhältnisse in Schwertern des Typs „Apa" und assoziierten Bronzeobjekten aus Apa, Nebra und Dänemark. In L. Glaser (Ed.), *Archäometrie und Denkmalpflege 2018, 20–24. März 2018, DESY, Hamburg, Deutschland* (pp. 64–67). Verlag Deutsches Elektronen-Synchrotron. https://doi.org/10.3204/DESY-PROC-2018-01

Buchwald, V. F. (2005). *Iron and steel in ancient times*. Historisk-filosofiske Skrifter 29. Royal Danish Academy of Sciences and Letters. Special-Trykkeriet Viborg a-s.

Buchwald, V. F., & Wivel, H. (1998). Slag analysis as a method for the characterization and provenancing of ancient iron objects. *Materials Characterization, 40*, 73–96. https://doi.org/10.1016/S1044-5803(97)00105-8

Canovaro, C., Angelini, I., Artioli, G., Nimis, P., & Borgna, E. (2019). Metal flow in the late Bronze Age across the Friuli-Venezia Giulia plain (Italy): New insights on Cervignano and Muscoli hoards by chemical and isotopic investigations. *Archaeological and Anthropological Sciences, 11*, 4829–4846. https://doi.org/10.1007/s12520-019-00827-2

Canovaro, C. (2016). Diffusion of Alpine copper in Friuli Venezia Giulia in the Middle-Late Bronze Age. PhD Dissertation. Universita degli Studi di Padova. https://www.research.unipd.it/handle/11577/3424443 Accessed 17 Apr 2022

Charlton, M. F., Blakelock, E., Martinón-Torres, M., & Young, T. (2012). Investigating the production provenance of iron artifacts with multivariate methods. *Journal of Archaeological Science, 39*, 2280–2293. https://doi.org/10.1016/j.jas.2012.02.037

Chugayev, A. V., Zaytseva, I., & Merkel, S. W. (2020). Lead isotopic characteristics and metal sources for the jewelry in the medieval rural settlements from the Suzdal Region (Kievan Rus'). *Metalla, 25*(2), 101–125. https://doi.org/10.46586/metalla.v25.2019.i2.101-125

Costa, K., Brun, P., & Mille, B. (2021). Late Bronze Age new statistical and archaeometallurgical artefacts surveys from France and Switzerland (950 to 800 BCE). In B. Török & A. Giumlia-Mair (Eds.), *Proceedings of the 5th International Conference "Archaeometallurgy in Europe"* (pp. 219–236). Editions Mergoil. https://halshs.archives-ouvertes.fr/halshs-03575131/ Accessed 1 Aug 2022

Coustures, M.-P., Beziat, D., & Tollon, F. (2003). The use of trace element analysis of entrapped slag inclusions to establish ore-bar iron links: Examples from two Galloroman iron-making sites in France (Les Martys, Montagne Noire, and Les Ferrys, Loiret). *Archaeometry, 45*, 599–613. https://doi.org/10.1046/j.1475-4754.2003.00131.x

Coustures, M.-P., Rico, C., Beziat, D., Djaoui, D., Long, L., Domergue, C., & Tollon F. (2006). La provenance des barres de fer romaines des Saintes-Maries de-la-Mer (Bouches-du-Rhône). Etude archéologique et archéométrique. *Gallia, 63*, 243–261. https://www.persee.fr/doc/galia_0016-4119_2006_num_63_1_3297 Accessed 28 Mar 2018

Cui, J., & Wu, X. (2011). An experimental investigation on lead isotope fractionation during metallurgical processes. *Archaeometry, 53*(1), 205–214. https://doi.org/10.1111/j.1475-4754.2010.00548.x

De Ceuster, S., & Degryse, P. (2020). A 'match-no match' numerical and graphical kernel density approach to interpreting lead isotope signatures of ancient artefacts. *Archaeometry, 62*, 107–116. https://doi.org/10.1111/arcm.12552

Dillmann, P., Schwab, R., Bauvais, S., Brauns, M., Disser, A., Leroy, S., Gassmann, G., & Fluzin, P. (2017). Circulation of iron products in the North-Alpine area during the end of the First Iron Age (6th-5th c. BC): A combination of chemical and isotopic approaches. *Journal of Archaeological Science, 87*, 108–124. https://doi.org/10.1016/j.jas.2017.10.002

Disser, A., Dillmann, P., Leroy, M., Merluzzo, P., & Leroy, S. (2016a). The bridge of Dieulouard (Meurthe-et-Moselle, France): A fresh perspective on metal supply strategies in Carolingian economy. *ArchéoSciences, 40*, 149–161. https://doi.org/10.4000/archeosciences.4830

Disser, A., Dillmann, P., Leroy, M., L'Héritier, M., Bauvais, S., & Fluzin, P. (2016b). Iron supply for the building of Metz Cathedral: New methodological development for provenance studies. *Archaeometry, 59*, 493–510. https://doi.org/10.1111/arcm.12265

Durali-Mueller, S., Brey, G. P., Wigg-Wolf, D., & Lahaye, Y. (2007). Roman lead mining in Germany: Its origin and development through time deduced from lead isotope provenance studies. *Journal of Archaeological Science, 34*(10), 1555–1567. https://doi.org/10.1016/j.jas.2006.11.009

Gale, N. H. (2009). A response to the paper of A. M. Pollard: What a long, strange trip it's been: Lead isotopes and archaeology. In A. J. Shortland, I. C. Freestone, & T. Rehren, T. (eds.) *From mine to microscope: Advances in the study of ancient technology* (pp. 191–196). Oxbow Books

Gavranović, M., Mehofer, M., Kapuran, A., Koledin, J., Mitrović, J., Papazovska, A., Pravidur, A., Đorđević, A., & Jacanović, D. (2022). Emergence of monopoly–copper exchange networks during the Late Bronze Age in the western and central Balkans. *PLoS ONE, 17*(3), e0263823. https://doi.org/10.1371/journal.pone.0263823

Gebhard, R. & Krause, R. (2020). Critical comments on the find complex of the so-called Nebra Sky Disk. *Archäologische Informationen, 43*, 325–346. https://journals.ub.uni-heidelberg.de/index.php/arch-inf/article/download/81419/75457. Accessed 25 Apr 2022

Glascock, M. D. (2016). Compositional analysis in archaeology. Oxford Handbooks. https://doi.org/10.1093/oxfordhb/9780199935413.013.8 Accessed 8 Aug 2021

Hsu, Y. K., Sabatini, B., Bayarkjuu, N., Turbat, T., Giscard, P.-H., & Klein, S. (2020). Discerning social interaction and cultural influence in Early Iron Age Mongolia through archaeometallurgical investigation. *Archaeological and Anthropological Sciences, 12*, 11. https://doi.org/10.1007/s12520-019-00952-y

Jouttijärvi, A. (2020). On slag inclusions in iron and provenancing in Northern Europe. In M. Brumlich, E. Lehnhardt, & M. Meyer (Eds.), *The Coming of Iron. The Beginnings of Iron Smelting in Central Europe. Proceedings of the International Conference Freie Universität Berlin Excellence Cluster 264 Topoi 19–21 October 2017* (pp. 37–50). Berliner Archäologische Forschungen 18. Verlag Marie Leidorf GmbH.

Killick, D. J., Stephens, J. A., & Fenn, T. R. (2020). Geological constraints on the use of lead isotopes for provenance in archaeology. *Archaeometry, 62*(S51), 86–105. https://doi.org/10.1111/arcm.12573

Klein, S., Rose, T., Westner, K. J., & Hsu, Y.-K. (2022). From OXALID to GlobaLID: Introducing a modern and FAIR lead isotope database with an interactive application. *Archaeometry, 64*(4), 1–16. https://doi.org/10.1111/arcm.12762

L'Héritier, M., Dillmann, P., & Sarah, G. (2020). Deciphering the iron provenance on a medieval building yard: The case of Bourges Cathedral. *Minerals, 10*(12), 1131. https://doi.org/10.3390/min10121131

Leroy, S., Cohen, S. X., Verna, C., Gratuze, B., Téreygeol, F., Fluzin, P., Bertrand, L., & Dillmann, P. (2012). The medieval iron market in Ariège (France). Multidisciplinary analytical approach and multivariate analyses. *Journal of Archaeological Science, 39*, 1080–1093. https://doi.org/10.1016/j.jas.2011.11.025

Leroy, S., Hendrickson, M., Bauvais, S., Vega, E., Blanchet, T., Disser, A., & Delque-Kolic, E. (2018). The ties that bind: Archaeometallurgical typology of architectural crampons as a method for reconstructing the iron economy of Angkor, Cambodia (tenth to thirteenth c.). *Archaeological and Anthropological Sciences, 10*, 2137–2157. https://doi.org/10.1007/s12520-017-0524-3

Ling, J., Hjärthner-Holdar, E., Grandin, L., Stos-Gale, Z., Kristiansen, K., Mehleim, A. L., Artioli, G., Angelini, I., Krause, R., & Canovaro, C. (2019). Moving metals IV: Swords, metal sources and trade networks in Bronze Age Europe. *Journal of Archaeological Science: Reports, 26*, 101837. https://doi.org/10.1016/j.jasrep.2019.05.002

Ling, J., Stos-Gale, Z., Grandin, L., Billstrom, K., Hjarthner-Holdar, E., & Persson, P.-O. (2014). Moving metals II: Provenancing Scandinavian Bronze Age artefacts by lead isotope and elemental analyses. *Journal of Archaeological Science, 41*, 106–132. https://doi.org/10.1016/j.jas.2013.07.018

Liritzis, J., Laskaris, N., Vafiadou, A., Karapanagiotis, I., Volonakis, P., Papageorgopoulou, C., & Bratitsi, M. (2020). Archaeometry: An overview. *Scientific Culture, 6*(1), 49–98. https://doi.org/10.5281/zenodo.3625220

Liu, Ch., Liu, R., Zhu, S., Wu, J., Pollard, A. M., Cui, J., Tong, J., Huan, L., & Hsu, Y. K. (2022). New scientific analyses reveal mixing of copper sources in the early Iron Age metal production at Ili, western China. *Archaeometry, 64*(S1), 88–115. https://doi.org/10.1111/arcm.12770

Liu, R. & Pollard, A.M. (2022). Asking different questions: Highly radiogenic lead, mixing and recycling of metal and social status in the Chinese Bronze Age, *Mineralogical Magazine*, 1-11. https://doi.org/10.1180/mgm.2022.32

Milot, J., Blichert-Toft, J., Ayarzagüena Sanz, M., Fetter, N., Télouk, Ph., & Albarède, F. (2021). The significance of galena Pb model ages and the formation of large Pb-Zn sedimentary deposits. *Chemical Geology, 583*, 120444. https://doi.org/10.1016/j.chemgeo.2021.120444

Mödlinger, M., & Trebsche, P. (2020). Archaeometallurgical investigation of a Late Bronze Age hoard from Mahrersdorf in Lower Austria. *Journal of Archaeological Science: Reports, 33*, 102476. https://doi.org/10.1016/j.jasrep.2020.102476

Mödlinger, M., Trebsche, P., & Sabatini, B. (2021). Melting, smelting, and recycling: A regional study around the Late Bronze Age mining site of Prigglitz-Gasteil Lower Austria. *Plos ONE, 16*(7), e0254096. https://doi.org/10.1371/journal.pone.0254096

Niederschlag, E., Pernicka, E., Seifert, Th., & Bartelheim, M. (2003). The determination of lead isotope ratios by multiple collector ICP-MS: A case study of early Bronze Age artefacts and their possible relation with ore deposits of the Erzgebirge. *Archaeometry, 45*, 61–100. https://doi.org/10.1111/1475-4754.00097

Nørgaard, H. W., Pernicka, E., & Vandkilde, H. (2021). Shifting networks and mixing metals: Changing metal trade routes to Scandinavia correlate with Neolithic and Bronze Age transformations. *PLoS ONE, 16*(6), e0252376. https://doi.org/10.1371/journal.pone.0252376

Nørgaard, H. W., Pernicka, E., & Vandkilde, H. (2019). On the trail of Scandinavia's early metallurgy: Provenance, transfer and mixing. *PLoS ONE, 14*(7), e0219574. https://doi.org/10.1371/journal.pone.0219574

Orfanou, V., Birch, T., Lichtenberger, A., Raja, R., Barfod, G. H., Lesher, C. E., & Eger, C. (2020). Copper-based metalwork in Roman to early Islamic Jerash (Jordan): Insights into production and recycling through alloy compositions and lead isotopes. *Journal of Archaeological Science: Reports, 33*, 102519. https://doi.org/10.1016/j.jasrep.2020.102519

Oudbashi, O., Renson, V., & Hasanpour, A. (2021). Lead isotope analysis of tin bronze objects from the Iron Age site at Baba Jilan, Luristan, western Iran. *Archaeological and Anthropological Sciences, 13*, 161. https://doi.org/10.1007/s12520-021-01428-8

Pernicka, E. (2014). Chapter 11. Provenance determination of archaeological metal objects. In B. W. Roberts, & C. Thornton (Eds.), *Archaeometry in Global Perspective. Methods and Syntheses* (pp. 239–268). Springer. https://doi.org/10.1007/978-1-4614-9017-3_11

Pernicka, E., Adam, J., Borg, G., Brügmann, G., Bunnefeld, J.-H., Kainz, W., Klamm, M., Koiki, T., Meller, H., Schwarz, R., Stöllner, T., Wunderlich, C.-H., & Reichenberger, A. (2020). Why the Nebra Sky Disc dates to the Early Bronze Age. An Overview of the Interdisciplinary Results. *Archaeologia Austriaca, 104*, 89–122. https://doi.org/10.1553/archaeologia104s89

Pernicka, E. (1990). Gewinnung und Verbreitung der Metalle in prähistorischer Zeit. *Jahrbuch des Römisch-Germanischen Zentralmuseums Mainz, 37*(1), 21–129. https://doi.org/10.11588/jrgzm.1990.1.72999

Pernicka, E., Lutz, J., & Stollner, T. (2016a). Bronze Age copper produced at Mitterberg, Austria, and its distribution. *Archaeologia Austriaca, 100*, 19–55. https://doi.org/10.1553/archaeologia100s19

Pernicka, E., Nessel, B., Mehofer, M., & Safta, E. (2016b). Lead isotope analyses of metal objects from the Apa hoard and other Early and Middle Bronze Age items from Romania. *Archaeologia Austriaca, 100*, 57–86. https://doi.org/10.1553/archaeologia100s57

Pollard, M. (2009). What a long, strange trip it's been: Lead isotopes and archaeology. In A. J. Shortland, I. C. Freestone, & T. Rehren, T. (eds.) *From mine to microscope: Advances in the study of ancient technology* (pp. 181–190). Oxbow Books

Pollard, A., Bray, P., Cuénod, A., Hommel, P., Hsu, Y., Liu, R., Perucchetti, L., Pouncett, J., & Saunders, M. (2018). Previous approaches to the chemistry and provenance of archaeological copper alloys. In iid. *Beyond provenance: New approaches to interpreting the chemistry of archaeological copper alloys* (pp. 13–40). Leuven University Press. https://doi.org/10.2307/j.ctv7xbs5r.4

Pollard, A. M., & Bray, P. J. (2015). A new method for combining lead isotope and lead abundance data to characterize archaeological copper alloys. *Archaeometry, 57*(6), 999–1008. https://doi.org/10.1111/arcm.12145

Pryce, T. O., Cadet, M., Allard, F., Kim, N. C., Hiep, T. J., Dung, L. T. M., Lang, W., & Foy, E. (2022). Copper-base metal supply during the northern Vietnamese Bronze and Iron Ages: Metallographic, elemental, and lead isotope data from Dai Trach, Thành Dên, Gò Mun, and Xuân Lâp. *Archaeological and Anthropological Sciences, 14*, 16. https://doi.org/10.1007/s12520-021-01489-9

Rademakers, F. W., Verly, G., Somaglino, C., & Degryse, P. (2020). Geochemical changes during Egyptian copper smelting? An experimental approach to the Ayn Soukhna process and broader implications for archaeometallurgy. *Journal of Archaeological Science, 122*, 105223. https://doi.org/10.1016/j.jas.2020.105223

Radivojević, M., Roberts, B. W., Pernicka, E., Stos-Gale, Z., Martinón-Torres, M., Rehren, T., Bray, B., Brandherm, D., Ling, J., Mei, J., Vandkilde, H., Kristiansen, K., Shennan, S. J., & Broodbank, C. (2019). The provenance, use, and circulation of metals in the European Bronze Age: The state of debate. *Journal of Archaeological Research, 27*, 131–186. https://doi.org/10.1007/s10814-018-9123-9

Scaife, B., Barreiro, B. A., McDonnell, J. G., & Pollard, A. M. (2008). Lead isotope ratios of 36 galenas from the Northern Pennines. Online source. http://www.brettscaife.net/lead/npennine/npennine1-2.html Accessed 25 Aug 2022

Schreiner, M. (2007). *Erzlagerstatten im Hrontal*. Verlag Marie Leidorf GmbH.

Schwab, R., Heger, D., Höppner, B., & Pernicka, E. (2006). The provenance of iron artefacts from Manching: A multitechnique approach. *Archaeometry, 48*, 433–452. https://doi.org/10.1111/j.1475-4754.2006.00265.x

Schwab, R., Brauns, M., Fasnacht, W., Womer Katzev, S., Lockhoff, N., & Wylde Swiny, H. (2022). From Cyprus, or to Cyprus? A pilot study with osmium isotopy and siderophile trace elements to reconstruct the origin of corroded iron billets from the Kyrenia shipwreck. *Journal of Archaeological Science: Reports, 42*, 103365. https://doi.org/10.1016/j.jasrep.2022.103365

Seeliger, T.C., Pernicka, E., Wagner, G. A., Begemann, F., Schmitt-Strecker, S., Eibner, C., Öztunali, Ö., & Baranyi, I. (1985). Archäometallurgische Untersuchungen in Nord- und Ostanatolien. *Jahrbuch des Römisch-Germanisches Zentralmuseums Mainz, 32*, 597–659. https://doi.org/10.11588/jrgzm.1985.0.69268

Siklósi, Z., & Szilágyi, M. (2019). New data on the provenance of copper finds from the Early-Middle Copper Age of the Great Hungarian Plain. *Archaeological and Anthropological Sciences, 11*, 5275–5285. https://doi.org/10.1007/s12520-019-00867-8

Standish, Ch. D., Merkel, S. W., Hsieh, Y.-T., & Kershaw, J. (2021). Simultaneous lead isotope ratio and gold-lead-bismuth concentration analysis of silver by laser ablation MC-ICP-MS. *Journal of Archaeological Science, 125*, 105229. https://doi.org/10.1016/j.jas.2020.105299

Stepanov, I. A., Artemyev, D. A., Naumov, A. M., Blinov, I. A., & Ankushev, M. N. (2021). Investigation of ancient iron and copper production remains from Irtyash Lake (middle Trans-Urals, Russia). *Journal of Archaeological Science: Reports, 40*, 103255. https://doi.org/10.1016/j.jasrep.2021.103255

Stos, Z. A. (2009). Across the wine dark seas... Sailor tinkers and royal cargoes in the Late Bronze Age eastern Mediterranean. In A. J. Shortland, I. C. Freestone, & T. Rehren (Eds.), *From mine to microscope. Advances in the study of ancient technology* (pp. 163–180). Oxbow Books. https://www.academia.edu/10144804 Accessed 15 Jul 2022

Tomczyk, C. (2022). A database of lead isotopic signatures of copper and lead ores for Europe and the Near East. *Journal of Archaeological Science, 146*, 105657. https://doi.org/10.1016/j.jas.2022.105657

Tomczyk, C., Costa, K., Desachy, B., Brun, P., & Petit, Ch. (2021a). Multivariate statistical study of lead isotopic data: Proposal of a protocol for provenance determination. In B. Török & A. Giumlia-Mair (Eds.), *Proceedings of the 5th International Conference "Archaeometallurgy in Europe"* (pp. 165–182). Editions Mergoil. https://halshs.archives-ouvertes.fr/halshs-03477904v1 Accessed 26 Mar 2022

Tomczyk, C., Costa, K., Giosa, A., Brun, P., & Petit, Ch. (2021b). Provenance studies using lead isotopy: Contribution of the consideration of geological contexts in archaeological databases. *Bulletin de la Société Géologique de France, 92*, 20. https://doi.org/10.1051/bsgf/2021008

Wagner, G.A., Pernicka, E., Seeliger, T.C., Lorenz, I. B., Begemann, F., Schmitt-Strecker, S., Eibner, C. & Öztunali, Ö. (1986) Geochemische und isotopische Charakteristika fruher Rohstoffquellen für Kupfer, Blei, Silber und Gold in der Turkei. *Jahrbuch des Römisch-Germanisches Zentralmuseums Mainz, 33,* 723–752. https://www.researchgate.net/publication/284509045 Accessed 30 Aug 2022

Wagner, G.A., Pernicka, E., Seeliger, T. C., Öztunali, Ö., Baranyi, I., Begemann, F., & Schmitt-Strecker, S. (1985). Geologische Untersuchungen zur frühen Metallurgie in NW-Anatolien. *Bulletin of the Mineral and Exploration Institute of Turkey, 100–101*, 45–81. https://dergipark.org.tr/tr/download/article-file/44533 Accessed 30 Aug 2022

Westner, K. J., Rose, T., Klein, S., & Hsu Y. K. (2021). GlobaLID – global lead isotope database. V. 1.0. GFZ Data Services. https://doi.org/10.5880/fidgeo.2021.031.

Wood, J. R. (2022). Approaches to interrogate the erased histories of recycled archaeological objects. *Archaeometry, 64*(S1), 187–205. https://doi.org/10.1111/arcm.12756

Wood, J. R. & Liu, Y. (2022). A multivariate approach to investigate metallurgical technology: The case of the Chinese ritual bronzes. *Journal of Archaeological Method and Theory*. https://doi.org/10.1007/s10816-022-09572-8

Wood, J. R., Montero-Ruiz, I., & Martinón-Torres, M. (2019). From Iberia to the Southern Levant: The movement of silver across the Mediterranean in the Early Iron Age. *Journal of World Prehistory, 32*, 1–31. https://doi.org/10.1007/s10963-018-09128-3

Żabiński, G., Gramacki, J., Gramacki, A., Mišta-Jakubowska, E. A., Birch, T., & Disser, A. (2020). Multi-classifier majority voting analyses in provenance studies on iron artefacts. *Journal of Archaeological Science, 113*, 105055. https://doi.org/10.1016/j.jas.2019.105055

Zeiler, M., Garner, J., & Golze, R. (2016). High medieval silver mining and non-ferrous metallurgy in Northern Siegerland, Germany. An Interim Report. *Metalla, 22*(2), 185–201. https://www.academia.edu/es/35232788/. Accessed 8 Sept 2022

Zeiler, M., Hucko, S., & Steffens, S. (2018). Stilvoll in die Krise – Die Grube Landeskrone bei Wilnsdorf im Siegerland. *Der Anschrift, 70*(1–2), 2–21. https://www.academia.edu/37627190/ Accessed 8 Sept 2022